
SEMF: Supervised Expectation-Maximization Framework for Predicting Intervals

Ilia Azizi*

HEC, University of Lausanne
Lausanne, Switzerland
ilia.azizi@unil.ch

Marc-Olivier Boldi

HEC, University of Lausanne
Lausanne, Switzerland
marc-olivier.boldi@unil.ch

Valérie Chavez-Demoulin

HEC, University of Lausanne
Expertise Center for Climate Extremes (ECCE)
Lausanne, Switzerland
valerie.chavez@unil.ch

Abstract

This work introduces the Supervised Expectation-Maximization Framework (SEMF), a versatile and model-agnostic framework that generates prediction intervals for datasets with complete or missing data. SEMF extends the Expectation-Maximization (EM) algorithm, traditionally used in unsupervised learning, to a supervised context, enabling it to extract latent representations for uncertainty estimation. The framework demonstrates robustness through extensive empirical evaluation across 11 tabular datasets, achieving—in some cases—narrower normalized prediction intervals and higher coverage than traditional quantile regression methods¹. Furthermore, SEMF integrates seamlessly with existing machine learning algorithms, such as gradient-boosted trees and neural networks, exemplifying its usefulness for real-world applications. The experimental results highlight SEMF’s potential to advance state-of-the-art techniques in uncertainty quantification.

1 Introduction

In the evolving field of machine learning (ML), the quest for models capable of predicting outcomes while quantifying the uncertainty of their predictions is critical. Estimating prediction uncertainty is particularly vital in high-stakes domains such as healthcare [1], finance [2], and autonomous systems [3], where prediction-based decisions can have significant consequences. Traditional approaches have primarily focused on point estimates, providing limited insight into the reliability of these predictions. This limitation underscores the necessity for frameworks that generate precise point predictions and robust prediction intervals. These intervals offer a range within which the true outcome is expected to lie with a specified probability, enabling a deeper understanding of prediction uncertainty. Consequently, research has increasingly focused on methodologies that extend beyond point estimation to include uncertainty quantification, thereby enhancing decision-making in applications that rely on predictive modeling [4].

In this paper, we introduce the Supervised Expectation-Maximization Framework (SEMF) based on the Expectation-Maximization (EM) algorithm [5]. Traditionally recognized as a clustering technique, EM is used for supervised learning in SEMF, allowing for both point estimates and prediction intervals using any ML model (model-agnostic). SEMF generates representations for latent

*Corresponding author.

¹Code: <https://github.com/Unco3892/semf-paper>

or missing modalities, making it particularly relevant for incomplete multi-modal data. This paper details the methodology behind the framework and proposes a training algorithm based on Monte Carlo (MC) sampling, also used in variational inference for Variational Auto-Encoders (VAEs) [6, 7]. Comparisons with other models across several datasets showcase its contribution to the existing uncertainty quantification and predictive modeling literature [8].

The remainder of this paper is organized as follows: Section 2 details the theory and the methodology of SEMF. Section 3 reviews related works in latent representation learning, uncertainty estimation, and handling of missing data. Section 4 describes the experimental setup, including datasets and evaluation metrics. Section 5 discusses the results, demonstrating the efficacy of SEMF. Lastly, Section 6 concludes the paper, and Section 7 outlines the limitations and potential research directions.

2 Method

This section presents the founding principles of SEMF from its parameters, training, and inference procedure with, at its core, the EM algorithm. This algorithm, first introduced by [5], is an unsupervised method for handling latent variables and incomplete data. Invented to maximize the model likelihood, it builds a sequence of parameters that guarantee an increase in the log-likelihood [9] by iterating between the Expectation (E) and the Maximization (M) steps. In the E-step, one computes

$$Q(p|p') = \mathbb{E}_{Z \sim p'(z|x)} [\log p(x, Z)] = \int \log p(x, z) p'(z|x) dz, \quad (1)$$

where p' stands for the current estimates, $\log p(x, z)$ is the log-likelihood of the complete observation (x, z) , and z is a latent variable. The M-step maximizes this Q -function: $p' \leftarrow \arg \max_p Q(p|p')$. The sequence is repeated until convergence.

The EM algorithm has already been used for supervised learning tasks using specific models [10–13], and, to the best of our knowledge, mainly focusing on point prediction through the use of Gaussian Mixture Models (GMMs). Our work differs by modifying the EM algorithm and MC sampling to generate prediction intervals with any ML model and, in theory, under any distribution. This results in SEMF, a framework consisting of an encoder-decoder architecture and a missing data simulator.

2.1 Problem Scenario

Let $x = (x_1, x_2, \dots, x_K)$ denote K inputs and the output be y . For simplicity, we limit y to be numerical, although it could be categorical without loss of generality. Component x_k is a source: a modality, a single or group of variables, or an unstructured input such as an image or text. For clarity, we limit to $K = 2$, where x_1 and x_2 are single variables. We assume that only x_1 may contain missing values, either at random or partially at random.

Let $p(y|x)$ be the density function of the outcome given the inputs (the fact that y is continuous can be easily relaxed). A founding assumption, in the spirit of VAE, is that $p(y|x)$ decomposes into $p(y|x) = \int p(y|z) p(z_1|x_1) p(z_2|x_2) dz_1 dz_2$, where $z = (z_1, z_2)$ are unobserved latent variables. We assume that $p(y|z, x) = p(y|z)$, that is, z contains all the information of x about y , and that $p(z|x) = p(z_1|x_1) p(z_2|x_2)$, that is, there is one latent variable per source. These are independent conditionally on their corresponding source. Finally, if x_1 is missing, then $p(y|x_2) = \int p(y|z) p(z_1|x_1) p(x_1|x_2) p(z_2|x_2) dx_1 dz_1 dz_2$. The contribution to the log-likelihood of a complete observation (y, z, x) is $\log p(y, z|x) = \log p(y|z) + \log p(z|x)$. In the E-step, we compute

$$\int \log p(y, z|x) p'(z|y, x) dz = \int \log p(y|z) p'(z|y, x) dz + \int \log p(z|x) p'(z|y, x) dz. \quad (2)$$

where p' is our current estimate. Eq. 2 can be estimated by MC sampling. Since sampling from $p'(z|y, x)$ can be inefficient, we rather rely on the decomposition $p'(z|y, x) = p'(y|z) p'(z|x) / p'(y|x)$. Thus, we sample z_r from $p'(z|x)$, $r = 1, \dots, R$, and, setting $w_r = p'(y|z_r) / \sum_t p'(y|z_t)$, approximate the right-hand side term of Eq. 2

$$\int \log p(y, z|x) p'(z|y) dz \approx \sum_{r=1}^R \{ \log p(y|z_r) + \log p(z_r|x) \} w_r. \quad (3)$$

If x_1 is missing, a similar development leads to

$$\int \log p(y, z, x_1|x_2) p'(z, x_1|y) dz \approx \sum_{r=1}^R \{\log p(y|z_r) + \log p(z_r|x) + \log p(x_{1,r}|x_2)\} w_r, \quad (4)$$

where $x_{1,r}$ and z_r are respectively sampled from $p'(x_1|x_2)$ and $p'(z|x_{1,r}, x_2)$.

2.2 Objective Function

Adapting Eq. 3 and Eq. 4 for the observed data $\{(y_i, x_i)\}_{i=1}^N$, the overall loss function, \mathcal{L} , is

$$\mathcal{L}(\phi, \theta, \xi) = - \sum_{i=1}^N \sum_{r=1}^R \{\log p_\phi(z_{i,r}|x_{i,r}) + \log p_\theta(y_i|z_{i,r}) + \mathbf{1}_{\{i \in I_m\}} \log p_\xi(x_{1,i,r}|x_{2,i})\} w_{i,r}, \quad (5)$$

where I_m is the set of those i 's such that $x_{1,i}$ is missing. The models of $p(y|z)$, $p(z|x)$, and $p(x_1|x_2)$ inherit parameters θ , ϕ , and ξ , respectively. Also, $x_{1,i,r}$ is sampled from $p_{\xi'}(x_1|x_{2,i})$, if $x_{1,i}$ is missing, and $z_{1,i,r}$ and $z_{2,i,r}$ are sampled from $p_{\phi'}(z_1|x_{1,i,r})$ and $p_{\phi'}(z_2|x_{2,i})$. Furthermore, for compactness of notation, $x_{i,r}$ is $(x_{1,i}, x_{2,i})$ if $x_{1,i}$ is observed, and $(x_{1,i,r}, x_{2,i})$ if $x_{1,i}$ is missing. Finally, the weights are

$$w_{i,r} = \frac{p_{\theta'}(y_i|z_{i,r})}{\sum_{t=1}^R p_{\theta'}(y_i|z_{i,t})}. \quad (6)$$

Eq. 5 shows that \mathcal{L} is a sum of losses associated with the encoder model, p_ϕ , for each source, the decoder model, p_θ , from the latent variables to the output, and, if applicable, the model handling missing data, p_ξ . At each M-step, \mathcal{L} is minimized with respect to θ , ϕ , and ξ . Then, θ' , ϕ' , and ξ' are updated, as well as the weights and the sampling. Then the process is iterated until convergence.

2.2.1 Example: $\mathcal{L}(\phi, \theta, \xi)$ under normality

Similar to [7], we develop further \mathcal{L} under normality assumptions for the encoder, p_ϕ , and the decoder, p_θ . These simple cases are illustrative, though any other distributions could be adopted, including non-continuous or non-numerical outcomes.

Encoder $p_\phi(z|x)$. Let m_k be the length of the latent variable z_k , $k = 1, 2$. We assume a normal model for Z_k given $X_k = x_k$,

$$Z_k|X_k = x_k \sim \mathcal{N}_{m_k}(g_{\phi_k}(x_k), \sigma_k^2 J_{m_k}), \quad (7)$$

where J_{m_k} is the $m_k \times m_k$ identity matrix. In particular,

$$\log p_\phi(z_k|x_k) = -\frac{m_k}{2} \log 2\pi - \frac{1}{2} \log \sigma_k^2 - \frac{1}{2\sigma_k^2} \sum_{j=1}^{m_k} \{z_{k,j} - g_{\phi_{k,j}}(x_k)\}^2, \quad k = 1, 2. \quad (8)$$

The mean $g_{\phi_k}(x_k)$ can be any model, such as a neural network, with output of length m_k , $k = 1, 2$. The scale σ_k can be fixed, computed via the weighted residuals, or learned through a separate set of models. It controls the amount of noise introduced in the latent dimension and is pivotal in determining the prediction interval width for $p(y|z)$. In this paper, σ_k is fixed for simplicity.

Decoder $p_\theta(y|z)$. We assume a normal model for Y given $Z = z$,

$$Y|Z = z \sim \mathcal{N}(f_\theta(z), \sigma^2). \quad (9)$$

This results in a log-likelihood contribution,

$$\log p_\theta(y|z) = -\frac{1}{2} \log 2\pi - \frac{1}{2} \log \sigma^2 - \frac{1}{2\sigma^2} \{y - f_\theta(z)\}^2. \quad (10)$$

Again, the mean $f_\theta(z)$ can be any model, such as a neural network.

Model for missing data $p_\xi(x_1|x_2)$. We use an empirical model for X_1 given $X_2 = x_2$ where $p_\xi(x_1|x_2)$ put masses only on those non-missing x_1 's in the training set. Let I_{nm} be the set of indices such that $x_{1,j}$, $j \in I_{nm}$, are all the non-missing x_1 in the training set. Additionally, for a given $j \in I_{nm}$, $x_1[j]$ is the observed x_1 corresponding to j . For a given x_2 , $p_\xi(x_2)$ is a vector of length $|I_{nm}|$, the cardinality of I_{nm} , with components

$$p_\xi(j|x_2) = \frac{\exp\{h_{\xi,j}(x_2)\}}{\sum_{t \in I_{nm}} \exp\{h_{\xi,t}(x_2)\}}, \quad j \in I_{nm}, \quad (11)$$

where h_ξ is a vector of length $|I_{nm}|$, typically a neural network with input x_2 and output on I_{nm} . Now, the probability of $X_1 = x_1$ given $X_2 = x_2$ is

$$p_\xi(x_1|x_2) = \sum_{j \in I_{nm}} p_\xi(j|x_2) \cdot \mathbb{1}\{x_1 = x_1^{(nm)}[j]\}. \quad (12)$$

Summary. Overall, the M-step is

$$\phi_k^* = \arg \min_{\phi_k} \sum_{i,r} w_{i,r} \sum_{j=1}^{m_k} \{z_{k,i,r,j} - g_{\phi_k,j}(x_{k,i,r})\}^2, \quad k = 1, 2, \quad (13)$$

$$\theta^* = \arg \min_{\theta} \sum_{i,r} w_{i,r} \{y_i - f_\theta(z_{i,r})\}^2, \quad (14)$$

$$(\sigma^*)^2 = \frac{1}{N} \sum_{i,r} w_{i,r} \{y_i - f_{\theta^*}(z_{i,r})\}^2, \quad (15)$$

$$\xi^* = \arg \max_{\xi} \sum_{t \in D_x} w_t \log p_\xi(j_t|x_{2,t}). \quad (16)$$

When $x_{1,i}$ is missing, the sampling is enriched by simulated $x_{1,i,r}$. Eq. 16 selects j^* from I_{nm} based on $p_{\xi^*}(j|x_2)$ according to Eq. 12 and Eq. 11. The above D_x is a subset of the data for ξ is only learned on the missing data part. After discussing the training steps in Subsection 2.3, the details are given in Algorithm 1 (Appendix A). We also note that the parameters above can be learned in parallel.

2.3 Training

For efficiency purpose, the training set, $\{1, \dots, N\}$, is segmented into batches $\{b_1, \dots, b_L\}$ on which the index i runs (and thus the denominator of Eq. 15 must be adapted accordingly). The process iterates for each batch until the maximum number of steps is reached or an early stopping criterion is satisfied. The framework requires tuning hyper-parameters such as the number of MC samples R , the number of latent nodes m_k , and the standard deviation σ_k of Z_k . Monitoring the point prediction on a hold-out validation is important to combat overfitting and terminate the training early with a PATIENCE hyper-parameter. Moreover, due to the generative nature of SEMF, the variation resulting from the initial random seed is measured in Subsection 4.2. Additionally, the model-specific hyper-parameters (p_ϕ , p_θ and p_ξ) are also discussed in the same Subsection.

2.4 Inference

The encoder-decoder structure of SEMF entails the simulations of z_r during inference, as depicted in Figure 1. In theory, any inference can be performed for \hat{y} , for instance the mean value $\hat{y} = \frac{1}{R} \sum_{r=1}^R f_\theta(z_r)$, where $z_r \sim p_\phi(z|x)$ (see Algorithm 2 in Appendix A). For prediction intervals, a double simulation scheme is used,

$$z_r \sim p(z|x), \quad \hat{y}_{r,s} \sim p_\theta(y|z_r), \quad r, s = 1, \dots, R. \quad (17)$$

Prediction interval at a given level of certainty α follows as

$$PI = \text{quantile} \left(\{\hat{y}_{r,s}\}; \frac{\alpha}{2}, 1 - \frac{\alpha}{2} \right). \quad (18)$$

Remark. We denote the R for inference as R_{infer} .

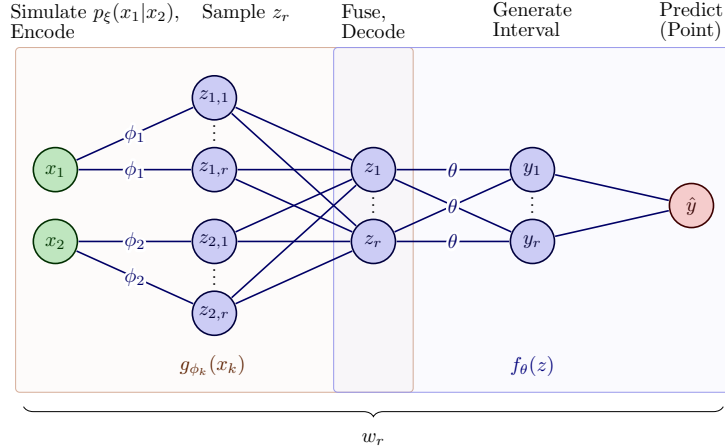


Figure 1: Inference procedure with the SEMF’s learnable parameters ϕ_k, θ and ξ . Here, we illustrate the number of inputs k as $k = 1, 2$, assuming that x_1 may contain missing values

3 Related Work

3.1 Latent Representation Learning

Latent representation learning involves modeling hidden variables from observed data for various ML tasks, most notably Auto-Encoders (AEs) and VAEs. AEs are neural networks reconstructing inputs by learning an intermediate latent representation. The leftmost part of AE is the encoder $g_\phi(\cdot)$, which embeds the input x into a latent variable z . It is passed to the rightmost part of AE, the decoder $f_\theta(\cdot)$, for the reconstruction $\hat{x} = f_\theta(z)$ of x through z . The parameters ϕ and θ are trained by minimizing the reconstruction loss. Unlike AEs, which focus on reconstruction, VAEs use variational methods to fit distributions of latent variables and of the output [7]. Given a sample x with a latent variable of z , VAEs learn the marginal likelihood, $p_\theta(x)$. Direct maximization of this likelihood is difficult [14]. Thus, alternative methods exist, such as maximizing the evidence lower bound (ELBO), which provides guarantees on the log-likelihood [15].

For supervised and semi-supervised tasks, latent representation learning can include task-specific predictions [16]. More specifically, models such as AEs follow the classical encoder-decoder objective while training a predictor $h_\psi(z)$ through an additional layer or model to estimate the output y . This dual objective helps in learning more task-relevant embeddings [17, 18]. Semi-supervised VAEs are similar, with the distinction that they couple the reconstruction loss of the unlabeled data with a variational approximation of latent variables. This is effective even with sparse labels [19, 20]. Similarly, the EM algorithm adapts well to minimal supervision [21] and using labeled and unlabeled data in semi-supervised settings for both single and multiple modalities [12, 22].

3.2 Prediction Intervals

Crucial for estimating uncertainty, prediction intervals in regression are often derived using methods such as Bayesian approaches [23–25], ensemble techniques [26, 27], or quantile regression [28, 29]. Additionally, these methods can be complemented with conformal prediction, a framework for calibrating any point predictor to produce prediction intervals [30, 31], making it highly relevant for enhancing reliability in applications requiring rigorous uncertainty quantification.

A key component of quantile regression is the pinball loss function, which effectively balances the residuals to capture the desired quantiles even for non-parametric models [32], making it ideal for asymmetric distributions where tail behavior is of critical importance [29]. This loss function is pivotal not only for single model scenarios but also enhances ensemble methods by refining their quantile estimate [33]. Conformal prediction further extends the applicability of these intervals by providing a layer of calibration that adjusts intervals obtained from any predictive model, ensuring they cover the true value with a pre-specified probability [34].

3.3 Missing Data

Managing missing values is a pivotal aspect when dealing with real-world data. Naive methods such as discarding instances or mean/median-imputation may be infeasible or carry the risk of changing the data distribution [35, 36] introducing bias if the missing values are not missing at random (MAR) or completely at random (MCAR). The chosen technique for handling missing data should adhere to the dataset’s characteristics and mechanisms behind the missing data [37].

More advanced approaches, like the Iterative Imputer from scikit-learn [38], an implementation of Multiple Imputation by Chained Equations (MICE) [39], expand on the simple imputations by iteratively modeling each feature with missing values as a function of other features [40, 41]. Due to its complexity, MICE is best compared with alternatives such as K-means clustering and artificial neural networks (ANNs). K-means assigns missing values based on cluster centroids [42] as opposed to ANNs, which learn complex, non-linear relationships between variables [43]. ANNs effectively predict or reconstruct missing values and thus are particularly useful in datasets where relationships between variables are intricate and not easily captured by straightforward imputation methods. Accordingly, ANNs have demonstrated superior performance over MICE and GMM (with EM for missing values) in scenarios where a large proportion of the data is missing [44].

4 Experimental Setup

4.1 Datasets

We systematically curate a subset of datasets from the OpenML-CTR23 [45] benchmark suite to evaluate and carry out our experiments. Initially comprising 35 datasets, we apply an exclusion criteria to refine this collection to 11 datasets. The details and overview are in Appendix B. We remove duplicated rows from all the datasets and carry out the standardization (scaling) of all predictors, including the outcome, which we transformed to have zero means and unit variances. The features of these datasets are then treated as separate inputs to SEMF. In the second stage of our experiments, we artificially introduce 50% missing values in our datasets for any predictor except for the first feature of a randomly chosen row, which emulates MAR or MCAR data. In all our datasets, 70% of the data is used to train all models, 15% as a hold-out validation set to monitor SEMF’s performance, and 15% to evaluate the models. To combat overfitting, baseline models that benefit from early stopping are allocated another 15% from the training data. Lastly, it is essential to note that all data in SEMF are processed batch-wise, without employing mini-batch training, to ensure consistency and stability in the training process.

4.2 Models

Our baseline consists of both point and quantile regression eXtreme Gradient Boosting (XGBoost) [46], Extremely Randomized Trees (ET) [47], and neural networks [48], depicted in Table 1. To ensure consistency in our experimental setup, we align the families and hyper-parameters of p_ϕ and p_θ with our baseline models. For example, in the case of XGBoost in SEMF, we use K XGBoost’s $g_{\phi_k}(x_k)$, one for each input x_k , $k = 1, \dots, K$, and one XGBoost for $f_\theta(z)$ with the same hyper-parameters. We refer to the SEMF’s adoption of these models as MultiXGBs, MultiETs, and MultiMLPs. When establishing prediction intervals, we set our uncertainty tolerance at 5% for both the baseline and SEMF (Eq. 18). The missing data simulator, p_ξ , is constructed using a shallow neural network, which employs the SELU activation function [49]. It is experimented with two distinct node counts: 50 and 100.

To constrain the breadth of our parameter exploration, the simulator for the missing model adopts the optimal set of hyper-parameters identified from analyses involving complete datasets. We target (larger) σ_k values that introduce more noise and produce better intervals than point predictions. The optimal models are then trained and tested with five different seeds, and the results are averaged. The point prediction, \hat{y} , uses the mean inferred values. We then study the performance of SEMF against mean and median imputation techniques, five nearest neighbors, and MICE from [38]. The imputers are used within the point and interval baseline models explained in the following subsection to form the missing value baseline. Appendix C contains more details on the hyper-parameters for each SEMF model and dataset.

Table 1: SEMF models, baselines, and hyper-parameters.

SEMF	Point Prediction Baseline	Interval Prediction Baseline
MultiXGBs	XGBoost [50] Trees: 100, Maximum depth: 5, Early stopping steps: 10	Quantile XGBoost Same as point prediction baseline, XGBoost
MultiETs	Extremely Randomized Trees [38] Trees: 100, Maximum depth: 10	Quantile Extremely Randomized Trees [51] Same as point prediction baseline, Extremely Randomized Trees
MultiMLPs	Deep Neural Network Hidden layers: 2, Nodes per layer: 100, Activation functions: ReLU, Epochs: 1000 or 5000, Learning rate: 0.001, Batch training, Early stopping steps: 100	Simultaneous Quantile Regression [48] Same as point prediction baseline, Deep Neural Network

4.3 Metrics

The evaluation of point predictions employs Root Mean Squared Error (RMSE), Mean Absolute Error (MAE), and R-squared (R^2). For prediction intervals, the chosen metrics, following [52, 53], are the Prediction Interval Coverage Probability (PICP), Mean Prediction Interval Width (MPIW), and Normalized Mean Prediction Interval Width (NMPIW) as described in Appendix D.1. This paper also evaluates SEMF on our new metric, termed Coverage-Width Ratio (CWR),

$$\text{CWR} = \frac{\text{PICP}}{\text{NMPIW}}, \quad (19)$$

which evaluates the coverage probability ratio to the prediction interval’s width. CWR provides a refined understanding of the balance between an interval’s accuracy (coverage) and precision (width). Though a larger value of this metric is better in higher confidence levels, the marginal increase in NMPIW is likely higher than that of PICP, resulting in decreasing CWR.

In our case, measuring the performance of SEMF over the baseline models is far more critical than reviewing absolute metrics in isolation. For any metric above, except for (R^2), this is computed as

$$\text{Metric}_{\Delta}(\%) = \left(\frac{\text{Metric}_{\text{SEMF}} - \text{Metric}_{\text{Baseline}}}{\text{Metric}_{\text{Baseline}}} \right) \times 100, \quad (20)$$

on which we base our decisions for selecting the best hyper-parameters as explained in Appendix D.2.

5 Results

We trained and tested 330 models corresponding to the three model types—MultiXGBs, MultiETs, and MultiMLPs—across 11 datasets with both complete and 50% missing data, with five seeds for each combination. Table 2 and Table 3 provide the mean and standard deviation for our metrics aggregated over the five seeds. All the results are in Appendix E. Below, we discuss the performances with complete data and with incomplete data.

5.1 Complete Data

The results of models with complete data are in Table 2. Overall, MultiXGBs and MultiMLPs performed generally well in producing intervals compared to their baselines as shown by positive ΔCWR and ΔPICP , notably, for instance, on *cpu_activity*, *naval_propulsion_plant*, and *energy_efficiency*. Interestingly, MultiMLPs also attained good relative performance improvements for point prediction, which can indicate that the chosen σ_k was too low for generating performant prediction intervals. MultiETs attained mixed results as, despite significant improvements in ΔCWR , it often failed to beat the baseline on ΔPICP .

Table 2: Test results for all models with complete data at 95% quantiles aggregated over five seeds. For each metric, the mean and standard deviation of the performance across the seeds are separated by \pm . Performance over the baseline is highlighted in bold.

DATASET	INTERVAL PREDICTIONS						POINT PREDICTIONS		
	RELATIVE			ABSOLUTE			RELATIVE		ABSOLUTE
	Δ CWR	Δ PICP	Δ NMPIW	PICP	MPIW	NMPIW	Δ RMSE	Δ MAE	R ²
MULTIXGBS									
SPACE_GA	-1%±6%	6%±2%	-7%±6%	0.89±0.01	1.80±0.12	0.20±0.01	-9%±1%	-10%±2%	0.60±0.01
CPU_ACTIVITY	25%±7%	9%±1%	12%±5%	0.89±0.01	0.37±0.01	0.07±0.00	21%±1%	-1%±3%	0.98±0.00
NAVAL_PROPULSION_PLANT	156%±15%	8%±1%	58%±2%	0.96±0.00	0.39±0.01	0.11±0.00	-14%±4%	-12%±2%	0.99±0.00
MIAMI_HOUSING	61%±6%	-7%±2%	43%±3%	0.82±0.01	0.45±0.01	0.06±0.00	4%±5%	3%±3%	0.91±0.01
KIN8NM	10%±3%	5%±2%	4%±4%	0.90±0.01	1.94±0.07	0.36±0.01	-20%±2%	-22%±2%	0.63±0.01
CONCRETE_COMPRESSIVE_STRENGTH	13%±5%	26%±6%	-11%±8%	0.91±0.01	1.25±0.03	0.25±0.01	-26%±7%	-40%±13%	0.85±0.01
CARS	18%±9%	15%±4%	2%±9%	0.89±0.02	0.70±0.05	0.12±0.01	-3%±3%	-1%±4%	0.95±0.00
ENERGY_EFFICIENCY	247%±99%	22%±7%	60%±20%	0.88±0.02	0.16±0.04	0.05±0.01	-15%±25%	-16%±19%	1.00±0.00
CALIFORNIA_HOUSING	31%±5%	0%±1%	23%±4%	0.88±0.01	1.17±0.02	0.28±0.00	-1%±1%	-1%±1%	0.81±0.00
AIRFOIL_SELF_NOISE	61%±45%	4%±10%	31%±18%	0.81±0.07	0.89±0.22	0.19±0.05	-64%±36%	-73%±46%	0.86±0.05
QSAR_FISH_TOXICITY	10%±4%	11%±4%	-1%±3%	0.76±0.01	1.46±0.03	0.23±0.00	3%±4%	1%±5%	0.55±0.02
MULTIETs									
SPACE_GA	9%±4%	-2%±1%	9%±4%	0.91±0.01	2.04±0.07	0.22±0.01	-16%±2%	-18%±3%	0.54±0.02
CPU_ACTIVITY	27%±3%	-8%±0%	27%±2%	0.90±0.01	0.47±0.01	0.09±0.00	-14%±2%	-20%±2%	0.98±0.00
NAVAL_PROPULSION_PLANT	219%±36%	-9%±0%	71%±3%	0.91±0.00	0.66±0.07	0.19±0.02	-320%±45%	-409%±40%	0.96±0.01
MIAMI_HOUSING	69%±4%	-13%±0%	48%±1%	0.86±0.00	0.65±0.02	0.08±0.00	-10%±2%	-20%±2%	0.90±0.00
KIN8NM	10%±2%	-9%±0%	17%±2%	0.88±0.01	2.27±0.05	0.44±0.01	-35%±2%	-38%±2%	0.48±0.01
CONCRETE_COMPRESSIVE_STRENGTH	9%±10%	-12%±2%	19%±9%	0.81±0.02	1.18±0.11	0.24±0.02	-67%±7%	-94%±10%	0.76±0.02
CARS	11%±7%	16%±2%	-5%±7%	0.83±0.02	0.53±0.04	0.09±0.01	3%±4%	1%±2%	0.95±0.00
ENERGY_EFFICIENCY	-4%±6%	0%±8%	-5%±15%	0.65±0.04	0.08±0.01	0.02±0.00	3%±4%	0%±2%	1.00±0.00
CALIFORNIA_HOUSING	31%±2%	-7%±0%	29%±1%	0.90±0.00	1.70±0.03	0.41±0.01	-15%±1%	-21%±1%	0.71±0.01
AIRFOIL_SELF_NOISE	18%±28%	-15%±5%	25%±18%	0.83±0.05	1.22±0.31	0.26±0.07	-117%±50%	-141%±57%	0.80±0.09
QSAR_FISH_TOXICITY	12%±2%	-9%±1%	19%±2%	0.82±0.01	1.81±0.02	0.28±0.00	-6%±1%	-11%±1%	0.53±0.01
MULTIMLPs									
SPACE_GA	8%±1%	0%±3%	7%±3%	0.81±0.02	1.25±0.02	0.14±0.00	0%±1%	-1%±1%	0.75±0.01
CPU_ACTIVITY	8%±3%	-9%±4%	15%±6%	0.72±0.02	0.24±0.01	0.05±0.00	7%±2%	5%±2%	0.98±0.00
NAVAL_PROPULSION_PLANT	21%±20%	0%±3%	16%±15%	0.92±0.01	0.22±0.03	0.07±0.01	-45%±28%	-36%±23%	1.00±0.00
MIAMI_HOUSING	9%±4%	2%±3%	6%±6%	0.81±0.02	0.41±0.03	0.05±0.00	-3%±2%	4%±2%	0.91±0.00
KIN8NM	2%±8%	8%±6%	-6%±12%	0.81±0.02	0.68±0.03	0.13±0.01	7%±3%	7%±2%	0.93±0.00
CONCRETE_COMPRESSIVE_STRENGTH	98%±15%	-23%±8%	61%±5%	0.56±0.04	0.28±0.01	0.06±0.00	12%±6%	15%±4%	0.91±0.01
CARS	0%±15%	6%±13%	-9%±3%	0.76±0.09	0.40±0.10	0.07±0.02	-3%±3%	0%±3%	0.95±0.00
ENERGY_EFFICIENCY	82%±20%	25%±26%	31%±12%	0.62±0.05	0.06±0.00	0.02±0.00	32%±4%	33%±3%	1.00±0.00
CALIFORNIA_HOUSING	-14%±3%	8%±1%	-26%±4%	0.89±0.01	1.31±0.02	0.31±0.01	7%±0%	9%±1%	0.82±0.00
AIRFOIL_SELF_NOISE	74%±46%	0%±7%	39%±17%	0.75±0.02	0.35±0.01	0.08±0.00	18%±4%	16%±5%	0.97±0.00
QSAR_FISH_TOXICITY	-6%±4%	11%±4%	-19%±5%	0.76±0.04	1.49±0.06	0.23±0.01	4%±5%	7%±5%	0.55±0.04

5.2 Missing Data

The results of models with 50% missing data are in Table 3. Note that relative metrics for SEMF are compared with the best result from any baseline imputer on that metric, regardless of how the imputer performed on the other metrics. Overall, the results are less consistent than with complete data. MultiXGBs maintained strong performance on some datasets, such as *naval_propulsion_plant*, but declined on others, like *cpu_activity*. MultiETs exhibited narrow predictions, improved absolute PICP in some cases, such as *energy_efficiency*, and improved relative point predictions. Conversely, MultiMLPs, while offering narrow prediction intervals, had higher PICP, indicating decreased predictive power and increased model uncertainty.

5.3 Discussion

The results indicate that specific models, particularly MultiXGBs, perform strongly with complete data. However, their robustness diminishes with increasing amounts of missing data. Further, we observe that MultiETs can produce narrow prediction intervals at the expense of reduced coverage. In contrast, despite the experiment design prioritizing interval estimation over point accuracy, MultiMLPs also deliver good point predictions. Precise choices, such as processing the columns separately, using the same hyper-parameters for both the complete and incomplete data, and fixing the same number of latent nodes per input (m_k), might have further constrained the models' ability to tailor their performance to varying dataset complexities.

The stability of SEMF across different seeds, as indicated by the absolute PICP and NMPIW, contrasts with the significant variability observed in baseline models, suggesting that SEMF offers a more reliable performance framework. The method's sampling operation, akin to cross-validation, helps combat overfitting, ensuring robust results despite variations in the data. Nonetheless, most models do not achieve the desired 95% prediction intervals. This shortfall could be addressed by integrating conformal prediction techniques with the intervals generated by SEMF, enhancing the reliability and coverage of prediction intervals across different datasets and missing data scenarios [34].

Table 3: Test results for all models with missing data at 95% quantiles aggregated over five seeds. For each metric, the mean and standard deviation of the performance across the seeds are separated by \pm . Performance over the baseline is highlighted in bold.

DATASET	INTERVAL PREDICTIONS						POINT PREDICTIONS		
	RELATIVE			ABSOLUTE			RELATIVE		ABSOLUTE
	Δ CWR	Δ PICP	Δ NMPIW	PICP	MPIW	NMPIW	Δ RMSE	Δ MAE	R ²
MULTIXGBS									
SPACE_GA	-5%±6%	4%±2%	-12%±7%	0.86±0.02	2.05±0.16	0.22±0.02	-7%±5%	-9%±3%	0.45±0.07
CPU_ACTIVITY	-5%±21%	12%±9%	-37%±52%	0.89±0.07	0.76±0.24	0.14±0.05	-1%±24%	-17%±14%	0.83±0.08
NAVAL_PROPULSION_PLANT	105%±33%	-16%±7%	56%±6%	0.70±0.07	0.62±0.06	0.18±0.02	-14%±22%	-29%±39%	0.77±0.06
MIAMI_HOUSING	16%±14%	-5%±6%	10%±18%	0.82±0.07	0.77±0.15	0.10±0.02	-14%±12%	-18%±11%	0.72±0.11
KIN8NM	-5%±2%	3%±2%	-14%±5%	0.88±0.01	2.46±0.07	0.48±0.01	-3%±3%	-4%±5%	0.40±0.02
CONCRETE_COMPRESSIVE_STRENGTH	2%±3%	8%±4%	-10%±4%	0.77±0.04	1.47±0.03	0.30±0.01	-16%±14%	-20%±16%	0.58±0.09
CARS	-15%±15%	26%±10%	-63%±29%	0.85±0.04	1.58±0.18	0.27±0.03	-30%±25%	-33%±27%	0.66±0.17
ENERGY_EFFICIENCY	10%±29%	11%±6%	-24%±48%	0.92±0.03	0.77±0.19	0.22±0.05	-186%±296%	-153%±210%	0.91±0.09
CALIFORNIA_HOUSING	26%±8%	-2%±3%	21%±7%	0.88±0.03	1.67±0.12	0.40±0.03	-4%±4%	-5%±5%	0.69±0.05
AIRFOIL_SELF_NOISE	-2%±21%	-3%±4%	-4%±19%	0.73±0.05	1.59±0.33	0.34±0.07	-37%±34%	-43%±40%	0.41±0.13
QSAR_FISH_TOXICITY	-2%±3%	0%±5%	-6%±8%	0.73±0.03	1.70±0.13	0.26±0.02	-4%±5%	-2%±4%	0.36±0.05
MULTIETS									
SPACE_GA	4%±4%	-5%±1%	7%±4%	0.88±0.02	2.23±0.10	0.24±0.01	-12%±4%	-14%±5%	0.40±0.06
CPU_ACTIVITY	-16%±12%	-5%±2%	-20%±21%	0.93±0.01	1.07±0.20	0.20±0.04	-30%±26%	-54%±22%	0.79±0.11
NAVAL_PROPULSION_PLANT	58%±5%	-17%±5%	46%±3%	0.82±0.05	1.38±0.10	0.41±0.03	-36%±23%	-93%±53%	0.71±0.06
MIAMI_HOUSING	20%±16%	-10%±5%	21%±14%	0.87±0.05	1.15±0.26	0.14±0.03	-27%±12%	-37%±12%	0.67±0.12
KIN8NM	5%±3%	-8%±2%	12%±4%	0.87±0.02	2.55±0.10	0.50±0.02	-11%±3%	-13%±3%	0.32±0.03
CONCRETE_COMPRESSIVE_STRENGTH	1%±6%	-14%±4%	13%±2%	0.80±0.02	1.83±0.06	0.37±0.01	-35%±23%	-50%±28%	0.49±0.07
CARS	-23%±7%	-8%±6%	-35%±16%	0.83±0.04	1.41±0.15	0.24±0.02	-33%±20%	-31%±20%	0.66±0.10
ENERGY_EFFICIENCY	-15%±18%	0%±10%	-36%±47%	0.85±0.06	0.51±0.05	0.15±0.01	-73%±89%	-84%±72%	0.94±0.04
CALIFORNIA_HOUSING	21%±7%	-7%±2%	22%±5%	0.91±0.02	2.19±0.13	0.52±0.03	-14%±3%	-17%±4%	0.61±0.06
AIRFOIL_SELF_NOISE	-7%±20%	-20%±2%	8%±18%	0.76±0.03	1.96±0.39	0.42±0.08	-65%±60%	-93%±78%	0.33±0.12
QSAR_FISH_TOXICITY	10%±8%	-9%±3%	16%±4%	0.82±0.04	2.12±0.20	0.33±0.03	-8%±9%	-10%±10%	0.39±0.10
MULTIMLPS									
SPACE_GA	-11%±6%	-15%±2%	1%±7%	0.68±0.04	1.44±0.09	0.16±0.01	-40%±26%	-34%±17%	0.21±0.25
CPU_ACTIVITY	-50%±18%	22%±16%	-193%±132%	0.86±0.11	0.97±0.42	0.18±0.08	-15%±21%	-23%±19%	0.75±0.14
NAVAL_PROPULSION_PLANT	-52%±21%	-14%±27%	-102%±62%	0.63±0.20	1.17±0.28	0.34±0.08	-108%±74%	-183%±218%	-0.03±0.53
MIAMI_HOUSING	-33%±17%	13%±11%	-92%±78%	0.85±0.06	0.99±0.32	0.12±0.04	-25%±9%	-28%±12%	0.67±0.11
KIN8NM	-11%±6%	-5%±2%	-8%±6%	0.77±0.01	1.76±0.09	0.35±0.02	-16%±9%	-15%±10%	0.37±0.04
CONCRETE_COMPRESSIVE_STRENGTH	-15%±14%	-13%±31%	-10%±54%	0.60±0.25	1.11±0.59	0.22±0.12	-12%±6%	-12%±7%	0.54±0.06
CARS	-51%±5%	43%±8%	-211%±38%	0.93±0.02	1.74±0.22	0.29±0.04	-28%±14%	-26%±15%	0.66±0.11
ENERGY_EFFICIENCY	-13%±20%	9%±17%	-30%±28%	0.66±0.15	0.33±0.15	0.09±0.04	1%±10%	-1%±18%	0.95±0.03
CALIFORNIA_HOUSING	-17%±7%	4%±4%	-28%±16%	0.88±0.03	1.84±0.17	0.44±0.04	-5%±3%	-3%±4%	0.61±0.06
AIRFOIL_SELF_NOISE	2%±18%	-2%±6%	-1%±23%	0.75±0.08	1.15±0.41	0.25±0.09	-15%±9%	-9%±9%	0.55±0.20
QSAR_FISH_TOXICITY	-17%±5%	6%±7%	-30%±12%	0.76±0.04	1.82±0.18	0.28±0.03	-13%±7%	-14%±9%	0.34±0.07

6 Conclusion

This paper introduces the Supervised Expectation-Maximization Framework (SEMF), a novel model-agnostic approach for generating prediction intervals in datasets with missing values. SEMF draws from the EM algorithm for supervised learning to devise latent representations that produce better prediction intervals than quantile regression. Due to SEMF’s iterative simulation technique, training and inference can be done with complete and incomplete data. A comprehensive set of 330 experimental runs on 11 datasets with three different model types showed that SEMF is superior to quantile regression, particularly for models such as XGBoost, which intrinsically lacks latent representations. This research underscores the potential of SEMF in various application domains and opens new avenues for further exploration for supervised latent representation learning and uncertainty estimation.

7 Limitations & Future Work

The primary limitation of this study was its reliance on the normality assumption, which may not fully capture the potential of SEMF across diverse data distributions. Although in Appendix F we demonstrate that the framework can learn non-normal patterns, further investigation and exploration of SEMF under other distributions, such as uniform and log-normal, are needed. The computational complexity of the approach presents another significant challenge, as the current implementation can be optimized for large-scale applications. Additionally, while the CWR metric is useful, it implicitly assumes that a 1% drop in PICP equates to a 1% reduction in NMPIW, thus assuming a uniform distribution. Evaluating CWR under various distributional assumptions would provide a more comprehensive assessment of its implications. Finally, applying the same hyper-parameters across all datasets without specific tuning for incomplete data likely contributes to the observed decline in accuracy and robustness.

Future work presents several intriguing avenues for exploration. A promising direction is the application of SEMF in multi-modal data settings, where the distinct p_ϕ components of the framework

could be adapted to process diverse data types—from images and text to tabular datasets—enabling a more nuanced and powerful approach to integrating heterogeneous data sources. This capability positions the framework as a versatile tool for addressing missing data challenges across various domains and can also help expand it to discrete and multiple outputs. Another valuable area for development is the exploration of methods to capture and leverage dependencies among input features, which could improve the model’s predictive performance and provide deeper insights into the underlying data structure. These advancements can enhance the broader appeal of end-to-end approaches like SEMF in the ML community.

References

- [1] Michael W. Dusenberry, Dustin Tran, Edward Choi, Jonas Kemp, Jeremy Nixon, Ghassen Jerfel, Katherine Heller, and Andrew M. Dai. Analyzing the role of model uncertainty for electronic health records. In *Proceedings of the ACM Conference on Health, Inference, and Learning*, CHIL ’20, page 204–213, New York, NY, USA, 2020. Association for Computing Machinery.
- [2] Wojciech Wisniewski, David Lindsay, and Sian Lindsay. Application of conformal prediction interval estimations to market makers’ net positions. In Alexander Gammerman, Vladimir Vovk, Zhiyuan Luo, Evgueni Smirnov, and Giovanni Cherubin, editors, *Proceedings of the Ninth Symposium on Conformal and Probabilistic Prediction and Applications*, volume 128 of *Proceedings of Machine Learning Research*, pages 285–301. PMLR, 09–11 Sep 2020.
- [3] Xiaolin Tang, Kai Yang, Hong Wang, Jiahang Wu, Yechen Qin, Wenhao Yu, and Dongpu Cao. Prediction-uncertainty-aware decision-making for autonomous vehicles. *IEEE Transactions on Intelligent Vehicles*, 7(4):849–862, 2022.
- [4] Zoubin Ghahramani. Probabilistic machine learning and artificial intelligence. *Nature*, 521(7553):452–459, 2015.
- [5] A. P. Dempster, N. M. Laird, and D. B. Rubin. Maximum likelihood from incomplete data via the em algorithm. *Journal of the Royal Statistical Society. Series B (Methodological)*, 39(1):1–38, 1977.
- [6] Alp Kucukelbir David M. Blei and Jon D. McAuliffe. Variational inference: A review for statisticians. *Journal of the American Statistical Association*, 112(518):859–877, 2017.
- [7] Diederik P. Kingma and Max Welling. Auto-Encoding Variational Bayes. In *2nd International Conference on Learning Representations, ICLR 2014, Banff, AB, Canada, April 14-16, 2014, Conference Track Proceedings*, 2014.
- [8] Jakob Gawlikowski, Cedrique Rovile Njiteucheu Tassi, Mohsin Ali, Jongseok Lee, Matthias Humt, Jianxiang Feng, Anna Kruspe, Rudolph Triebel, Peter Jung, Ribana Roscher, et al. A survey of uncertainty in deep neural networks. *Artificial Intelligence Review*, 56(Suppl 1):1513–1589, 2023.
- [9] CF Jeff Wu. On the convergence properties of the em algorithm. *The Annals of statistics*, pages 95–103, 1983.
- [10] Zoubin Ghahramani and Michael Jordan. Supervised learning from incomplete data via an em approach. In J. Cowan, G. Tesauro, and J. Alspecter, editors, *Advances in Neural Information Processing Systems*, volume 6. Morgan-Kaufmann, 1993.
- [11] David Williams, Xuejun Liao, Ya Xue, and Lawrence Carin. Incomplete-data classification using logistic regression. In *Proceedings of the 22nd International Conference on Machine Learning*, ICML ’05, page 972–979, New York, NY, USA, 2005. Association for Computing Machinery.
- [12] Wenchong He and Zhe Jiang. Semi-supervised learning with the em algorithm: A comparative study between unstructured and structured prediction. *IEEE Transactions on Knowledge and Data Engineering*, 34(6):2912–2920, 2022.

- [13] Robin Louiset, Pietro Gori, Benoit Dufumier, Josselin Houenou, Antoine Grigis, and Edouard Duchesnay. Ucs! : A machine learning expectation-maximization framework for unsupervised clustering driven by supervised learning. In *Machine Learning and Knowledge Discovery in Databases. Research Track: European Conference, ECML PKDD 2021, Bilbao, Spain, September 13–17, 2021, Proceedings, Part I 21*, pages 755–771. Springer, 2021.
- [14] Alp Kucukelbir David M. Blei and Jon D. McAuliffe. Variational inference: A review for statisticians. *Journal of the American Statistical Association*, 112(518):859–877, 2017.
- [15] Sivaraman Balakrishnan, Martin J. Wainwright, and Bin Yu. Statistical guarantees for the EM algorithm: From population to sample-based analysis. *The Annals of Statistics*, 45(1):77 – 120, 2017.
- [16] Durk P Kingma, Shakir Mohamed, Danilo Jimenez Rezende, and Max Welling. Semi-supervised learning with deep generative models. *Advances in neural information processing systems*, 27, 2014.
- [17] Fuzhen Zhuang, Xiaohu Cheng, Ping Luo, Sinno Jialin Pan, and Qing He. Supervised representation learning: transfer learning with deep autoencoders. In *Twenty-fourth international joint conference on artificial intelligence, IJCAI’15*, page 4119–4125. AAAI Press, 2015.
- [18] Lei Le, Andrew Patterson, and Martha White. Supervised autoencoders: Improving generalization performance with unsupervised regularizers. *Advances in neural information processing systems*, 31, 2018.
- [19] Tianchen Ji, Srikanth Vuppala, Girish V. Chowdhary, and K. Driggs-Campbell. Multi-modal anomaly detection for unstructured and uncertain environments. In *Conference on Robot Learning*, 2020.
- [20] Yilin Zhuang, Zhuobin Zhou, Burak Alakent, and Mehmet Mercangöz. Semi-supervised variational autoencoders for regression: Application to soft sensors. In *2023 IEEE 21st International Conference on Industrial Informatics (INDIN)*, pages 1–8, 2023.
- [21] Zhekun Luo, Devin Guillory, Baifeng Shi, Wei Ke, Fang Wan, Trevor Darrell, and Huijuan Xu. Weakly-supervised action localization with expectation-maximization multi-instance learning. In *Computer Vision–ECCV 2020: 16th European Conference, Glasgow, UK, August 23–28, 2020, Proceedings, Part XXIX 16*, pages 729–745. Springer, 2020.
- [22] Moucheng Xu, Yukun Zhou, Chen Jin, Marius de Groot, Daniel C Alexander, Neil P Oxtoby, Yipeng Hu, and Joseph Jacob. Expectation maximization pseudo labels. *Medical Image Analysis*, page 103125, 2024.
- [23] Christopher Williams and Carl Rasmussen. Gaussian processes for regression. *Advances in neural information processing systems*, 8, 1995.
- [24] James Hensman, Alexander Matthews, and Zoubin Ghahramani. Scalable variational gaussian process classification. In *Artificial Intelligence and Statistics*, pages 351–360. PMLR, 2015.
- [25] Yarin Gal and Zoubin Ghahramani. Dropout as a bayesian approximation: Representing model uncertainty in deep learning. In Maria Florina Balcan and Kilian Q. Weinberger, editors, *Proceedings of The 33rd International Conference on Machine Learning*, volume 48 of *Proceedings of Machine Learning Research*, pages 1050–1059, New York, New York, USA, 20–22 Jun 2016. PMLR.
- [26] Leo Breiman. Random forests. *Machine learning*, 45:5–32, 2001.
- [27] Balaji Lakshminarayanan, Alexander Pritzel, and Charles Blundell. Simple and scalable predictive uncertainty estimation using deep ensembles. *Advances in neural information processing systems*, 30, 2017.
- [28] Roger Koenker and Gilbert Bassett. Regression quantiles. *Econometrica*, 46(1):33–50, 1978.
- [29] Roger Koenker and Kevin F. Hallock. Quantile regression. *The Journal of Economic Perspectives*, 15(4):143–156, 2001.

- [30] Vladimir Vovk, Alexander Gammerman, and Glenn Shafer. *Algorithmic learning in a random world*, volume 29. Springer, 2005.
- [31] Vladimir Vovk, Alexander Gammerman, and Glenn Shafer. Conformal prediction: General case and regression. In *Algorithmic Learning in a Random World*, pages 19–69. Springer, 2022.
- [32] Ingo Steinwart and Andreas Christmann. Estimating conditional quantiles with the help of the pinball loss. *Bernoulli*, 17(1), February 2011.
- [33] Nicolai Meinshausen and Greg Ridgeway. Quantile regression forests. *Journal of machine learning research*, 7(6), 2006.
- [34] Yaniv Romano, Evan Patterson, and Emmanuel Candes. Conformalized quantile regression. In H. Wallach, H. Larochelle, A. Beygelzimer, F. d'Alché-Buc, E. Fox, and R. Garnett, editors, *Advances in Neural Information Processing Systems*, volume 32. Curran Associates, Inc., 2019.
- [35] Jinsung Yoon, Yao Zhang, James Jordon, and Mihaela van der Schaar. Vime: Extending the success of self- and semi-supervised learning to tabular domain. In H. Larochelle, M. Ranzato, R. Hadsell, M.F. Balcan, and H. Lin, editors, *Advances in Neural Information Processing Systems*, volume 33, pages 11033–11043. Curran Associates, Inc., 2020.
- [36] Anil Jadhav, Dhanya Pramod, and Krishnan Ramanathan. Comparison of performance of data imputation methods for numeric dataset. *Applied Artificial Intelligence*, 33(10):913–933, 2019.
- [37] Joseph G Ibrahim, Hongtu Zhu, and Niansheng Tang. Model selection criteria for missing-data problems using the em algorithm. *Journal of the American Statistical Association*, 103(484):1648–1658, 2008.
- [38] F. Pedregosa, G. Varoquaux, A. Gramfort, V. Michel, B. Thirion, O. Grisel, M. Blondel, P. Prettenhofer, R. Weiss, V. Dubourg, J. Vanderplas, A. Passos, D. Cournapeau, M. Brucher, M. Perrot, and E. Duchesnay. Scikit-learn: Machine learning in Python. *Journal of Machine Learning Research*, 12:2825–2830, 2011.
- [39] Stef van Buuren and Karin Groothuis-Oudshoorn. mice: Multivariate imputation by chained equations in r. *Journal of Statistical Software*, 45(3):1–67, 2011.
- [40] S. F. Buck. A method of estimation of missing values in multivariate data suitable for use with an electronic computer. *Journal of the Royal Statistical Society. Series B (Methodological)*, 22(2):302–306, 1960.
- [41] Joseph L Schafer. *Analysis of incomplete multivariate data*. CRC press, 1997.
- [42] Siwei Wang, Miaomiao Li, Ning Hu, En Zhu, Jingtao Hu, Xinwang Liu, and Jianping Yin. K-means clustering with incomplete data. *IEEE Access*, 7:69162–69171, 2019.
- [43] Ricardo Cardoso Pereira, Miriam Seoane Santos, Pedro Pereira Rodrigues, and Pedro Henriques Abreu. Reviewing autoencoders for missing data imputation: Technical trends, applications and outcomes. *Journal of Artificial Intelligence Research*, 69:1255–1285, 2020.
- [44] Marek Śmieja, Łukasz Struski, Jacek Tabor, Bartosz Zieliński, and Przemysław Spurek. Processing of missing data by neural networks. *Advances in neural information processing systems*, 31, 2018.
- [45] Sebastian Felix Fischer, Matthias Feurer, and Bernd Bischl. OpenML-CTR23 – a curated tabular regression benchmarking suite. In *AutoML Conference 2023 (Workshop)*, 2023.
- [46] Tianqi Chen and Carlos Guestrin. XGBoost: A scalable tree boosting system. In *Proceedings of the 22nd ACM SIGKDD International Conference on Knowledge Discovery and Data Mining*, KDD '16, pages 785–794, New York, NY, USA, 2016. ACM.
- [47] Pierre Geurts, Damien Ernst, and Louis Wehenkel. Extremely randomized trees. *Machine learning*, 63:3–42, 2006.
- [48] Natasa Tagasovska and David Lopez-Paz. Single-model uncertainties for deep learning. *Advances in Neural Information Processing Systems*, 32, 2019.

- [49] Günter Klambauer, Thomas Unterthiner, Andreas Mayr, and Sepp Hochreiter. Self-normalizing neural networks. *Advances in neural information processing systems*, 30, 2017.
- [50] Tianqi Chen and Carlos Guestrin. Xgboost: A scalable tree boosting system. In *Proceedings of the 22nd acm sigkdd international conference on knowledge discovery and data mining*, pages 785–794, 2016.
- [51] Reid A. Johnson. quantile-forest: A python package for quantile regression forests. *Journal of Open Source Software*, 9(93):5976, 2024.
- [52] Tim Pearce, Alexandra Brintrup, Mohamed Zaki, and Andy Neely. High-quality prediction intervals for deep learning: A distribution-free, ensembled approach. In *International conference on machine learning*, pages 4075–4084. PMLR, 2018.
- [53] Ting Zhou, Yuxin Jie, Yingjie Wei, Yanyi Zhang, and Hui Chen. A real-time prediction interval correction method with an unscented kalman filter for settlement monitoring of a power station dam. *Scientific Reports*, 13(1):4055, 2023.
- [54] Kaggle. Moneyball dataset. <https://www.kaggle.com/datasets/wduckett/moneyball-mlb-stats-19622012>, 2017. Accessed: 2024-02-02.
- [55] R. Kelley Pace and Ronald Barry. Quick computation of spatial autoregressive estimators. *Geographical Analysis*, 29(3):232–247, 1997.
- [56] C. Rasmussen, R. Neal, G. Hinton, D. van Camp, M. Revow, Z. Ghahramani, R. Kustra, and R. Tibshirani. Computer activity dataset. <http://www.cs.toronto.edu/~delve/data/datasets.html>, 1996. Accessed: 2024-02-02.
- [57] Andrea Coraddu, Luca Oneto, Aessandro Ghio, Stefano Savio, Davide Anguita, and Massimo Figari. Machine learning approaches for improving condition-based maintenance of naval propulsion plants. *Proceedings of the Institution of Mechanical Engineers, Part M: Journal of Engineering for the Maritime Environment*, 230(1):136–153, 2016.
- [58] Kaggle. Miami housing dataset. <https://www.kaggle.com/datasets/deepcontractor/miami-housing-dataset>, 2022. Accessed: 2024-02-02.
- [59] Z. Ghahramani. The kin datasets. <https://www.cs.toronto.edu/~delve/data/kin/desc.html>, 1996. Accessed: 2024-02-02.
- [60] I.-C. Yeh. Modeling of strength of high-performance concrete using artificial neural networks. *Cement and Concrete Research*, 28(12):1797–1808, 1998.
- [61] Shonda Kuiper. Introduction to multiple regression: How much is your car worth? *Journal of Statistics Education*, 16(3), 2008.
- [62] Athanasios Tsanas and Angeliki Xifara. Accurate quantitative estimation of energy performance of residential buildings using statistical machine learning tools. *Energy and Buildings*, 49:560–567, 2012.
- [63] R. Kelley Pace and Ronald Barry. Sparse spatial autoregressions. *Statistics & Probability Letters*, 33(3):291–297, 1997.
- [64] Thomas Brooks, Dennis Pope, and Michael Marcolini. Airfoil self-noise and prediction. NASA Technical Report 1218, NASA, 1989.
- [65] R. Todeschini M. Cassotti, D. Ballabio and V. Consonni. A similarity-based qsar model for predicting acute toxicity towards the fathead minnow (*pimephales promelas*). *SAR and QSAR in Environmental Research*, 26(3):217–243, 2015. PMID: 25780951.
- [66] Lukas Biewald. Experiment tracking with weights and biases, 2020. Software available from wandb.com.

A SEMF algorithm

Algorithm 1 SEMF Training: two input sources where x_1 can be missing

Require: y, x_1, x_2, R

Ensure: $\theta, \phi_1, \phi_2, \xi$

- 1: Initialize $\theta, \phi_1, \phi_2, \xi$
- 2: Initialize $D_y, D_{z_1}, D_{z_2}, D_x, D_i$ to \emptyset
- 3: Split $I = \{1, \dots, N\}$ into L batches $\{b_1, \dots, b_L\}$
- 4: **for** $\ell = 1, \dots, L$ **do**
- 5: **for all** i in b_ℓ **do**
- 6: **if** $x_{1,i}$ is absent **then**
- 7: **for** $r = 1, \dots, R$ **do**
- 8: Simulate $[j_{i,r}, x_{1,i,r}] \sim p_\xi(\cdot | x_{2,i})$
- 9: Simulate $z_{1,i,r} \sim p_{\phi_1}(\cdot | x_{1,i,r})$
- 10: Simulate $z_{2,i,r} \sim p_{\phi_2}(\cdot | x_{2,i})$
- 11: Set $z_{i,r} = [z_{1,i,r}, z_{2,i,r}]$
- 12: **end for**
- 13: **else**
- 14: **for** $r = 1, \dots, R$ **do**
- 15: Simulate $z_{1,i,r} \sim p_{\phi_1}(\cdot | x_{1,i})$
- 16: Simulate $z_{2,i,r} \sim p_{\phi_2}(\cdot | x_{2,i})$
- 17: Set $z_{i,r} = [z_{1,i,r}, z_{2,i,r}]$
- 18: **end for**
- 19: **end if**
- 20: **for** $r = 1, \dots, R$ **do**
- 21: Compute

$$w_{i,r} = \frac{p_\theta(y_i | z_{i,r})}{\sum_{t=1}^R p_\theta(y_i | z_{i,t})}$$

- 22: Update $D_y \leftarrow D_y \cup [y_i | z_{i,r} | w_{i,r}]$
- 23: Update $D_{z_2} \leftarrow D_{z_2} \cup [z_{2,i,r} | x_{2,i} | w_{i,r}]$
- 24: **if** $x_{1,i}$ is absent **then**
- 25: Update $D_{z_1} \leftarrow D_{z_1} \cup [z_{1,i,r} | x_{1,i,r} | w_{i,r}]$
- 26: Update $D_x \leftarrow D_x \cup [j_{i,r} | x_{2,i} | w_{i,r}]$
- 27: **else**
- 28: Update $D_{z_1} \leftarrow D_{z_1} \cup [z_{1,i,r} | x_{1,i} | w_{i,r}]$
- 29: **end if**
- 30: **end for**
- 31: Update $\theta \leftarrow Q_y(\theta, D_y)$
- 32: Update $\phi_1 \leftarrow Q_1(\phi_1, D_{z_1})$
- 33: Update $\phi_2 \leftarrow Q_2(\phi_2, D_{z_2})$
- 34: Update $\xi \leftarrow Q_x(\xi, D_x)$
- 35: **end for**
- 36: **end for**
- 37: Check convergence; Go to step 4 if not

Algorithm 2 SEMF Inference

Require: $\theta^*, \phi_1^*, \phi_2^*, \xi^*, x_1, x_2, R$ **Ensure:** $z_{i,r}$

```
1: for  $r = 1, \dots, R$  do
2:   if  $x_{1,i}$  is absent then
3:     Simulate  $[j_{i,r}, x_{1,i,r}] \sim p_{\xi^*}(\cdot | x_{2,i})$ 
4:     Simulate  $z_{1,i,r} \sim p_{\phi_1^*}(\cdot | x_{1,i,r})$ 
5:     Simulate  $z_{2,i,r} \sim p_{\phi_2^*}(\cdot | x_{2,i})$ 
6:     Set  $z_{i,r} = [z_{1,i,r}, z_{2,i,r}]$ 
7:   else
8:     Simulate  $z_{1,i,r} \sim p_{\phi_1^*}(\cdot | x_{1,i})$ 
9:     Simulate  $z_{2,i,r} \sim p_{\phi_2^*}(\cdot | x_{2,i})$ 
10:    Set  $z_{i,r} = [z_{1,i,r}, z_{2,i,r}]$ 
11:   end if
12: end for
```

B Datasets for tabular benchmark

OpenML-CTR23 [45] datasets are selected in the following manner. The first criterion is to exclude datasets exceeding 30,000 instances or 30 features to maintain computational tractability. Moreover, we exclude the *moneyball* data [54] to control for missing values and any datasets with non-numeric features, such as those with temporal or ordinal data not encoded numerically. We then categorize the datasets based on size: small for those with less than ten features, medium for 10 to 19 features, and large for 20 to 29 features. We apply a similar size classification based on the number of instances, considering datasets with more than 10,000 instances as large. To avoid computational constraints, we exclude datasets that were large in both features and instances, ensuring a varied yet manageable set for our experiments. This leads us to the final list of 11 datasets listed in Table 4.

Table 4: Summary of benchmark tabular datasets retained from [45]

DATASET NAME	N SAMPLES	N FEATURES	OPENML DATA ID	Y [MIN:MAX]	SOURCE
SPACE_GA	3,107	7	45402	[-3.06:0.1]	[55]
CPU_ACTIVITY	8,192	22	44978	[0:99]	[56]
NAVAL_PROPULSION_PLANT	11,934	15	44969	[0.95:1.0]	[57]
MIAMI_HOUSING	13,932	16	44983	[72,000:2,650,000]	[58]
KIN8NM	8,192	9	44980	[0.04:1.46]	[59]
CONCRETE_COMPRESSIVE_STRENGTH	1,030	9	44959	[2.33:82.6]	[60]
CARS	804	18	44994	[8,639:70,756]	[61]
ENERGY_EFFICIENCY	768	9	44960	[6.01:43.1]	[62]
CALIFORNIA_HOUSING	20,640	9	44977	[14,999:500,001]	[63]
AIRFOIL_SELF_NOISE	1,503	6	44957	[103.38:140.98]	[64]
QSAR_FISH_TOXICITY	908	7	44970	[0.053:9.612]	[65]

C Optimal set of hyper-parameters

The hyper-parameter tuning for SEMF is implemented and monitored using Weights & Biases [66]. A random search is done in the hyper-parameter space for a maximum of 500 iterations on all 11 datasets, focusing on tuning the models only on the complete datasets. Key hyper-parameters are varied across a predefined set to balance accuracy and computational efficiency. The following grid is used for hyper-parameter tuning: the number of importance sampling operations $R \in \{5, 10, 25, 50, 100\}$ (100 is omitted for MultiMLPS), nodes per latent dimension $m_k \in \{1, 5, 10, 20, 30\}$, and standard deviations $\sigma_{m_k} \in \{0.001, 0.01, 0.1, 1.0\}$. Early stopping steps (PATIENCE) are set to five or ten, and R_{infer} is explored at [30, 50, 70]. The option to run the models in parallel must be consistently enabled. Table 5 shows the optimal set of hyper-parameters. This table includes common hyper-parameters for complete and 50% datasets and another part showing ξ_{nodes} , which is tuned manually and only relevant to the missing data.

Table 5: Hyper-parameters for MultiXGBs, MultiETs, and MultiMLPs used for both complete and missing data.

DATASET	COMPLETE AND MISSING					MISSING
	R	m_k	σ_k	PATIENCE	R_{infer}	ξ_{nodes}
MULTIXGBs						
SPACE_GA	10	30	1.0	5	70	100
CPU_ACTIVITY	5	30	1.0	5	70	50
NAVAL_PROPULSION_PLANT	5	30	0.01	5	50	100
MIAMI_HOUSING	5	10	0.1	5	50	50
KIN8NM	5	30	1.0	10	70	100
CONCRETE_COMPRESSIVE_STRENGTH	25	30	1.0	5	70	100
CARS	50	10	1.0	10	70	100
ENERGY_EFFICIENCY	5	1	0.01	10	70	100
CALIFORNIA_HOUSING	5	10	0.1	10	50	100
AIRFOIL_SELF_NOISE	25	1	0.01	10	70	100
QSAR_FISH_TOXICITY	50	30	1.0	5	70	100
MULTIETs						
SPACE_GA	10	30	1.0	10	70	100
CPU_ACTIVITY	5	30	1.0	10	70	50
NAVAL_PROPULSION_PLANT	5	30	0.01	10	50	100
MIAMI_HOUSING	10	10	0.1	10	50	50
KIN8NM	5	30	1.0	10	70	100
CONCRETE_COMPRESSIVE_STRENGTH	25	30	1.0	10	70	100
CARS	100	5	0.1	10	100	100
ENERGY_EFFICIENCY	5	1	0.01	10	70	100
CALIFORNIA_HOUSING	5	10	0.1	5	50	100
AIRFOIL_SELF_NOISE	25	1	0.01	10	70	100
QSAR_FISH_TOXICITY	50	30	1.0	10	70	100
MULTIMLPs						
SPACE_GA	25	10	0.001	10	50	100
CPU_ACTIVITY	5	20	0.001	5	50	50
NAVAL_PROPULSION_PLANT	5	20	0.001	5	50	100
MIAMI_HOUSING	5	20	0.01	5	50	50
KIN8NM	5	20	0.001	5	50	100
CONCRETE_COMPRESSIVE_STRENGTH	5	30	0.001	10	50	100
CARS	5	30	0.1	5	50	100
ENERGY_EFFICIENCY	50	30	0.1	10	50	100
CALIFORNIA_HOUSING	5	20	0.01	5	50	100
AIRFOIL_SELF_NOISE	25	10	0.01	10	50	100
QSAR_FISH_TOXICITY	50	30	1.0	10	70	100

MultiXGBs and MultiMLPs benefit from early stopping to reduce computation time in complete and incomplete cases. Similarly, the baseline models for these instances use the same hyper-parameters for early stopping. Further, the number of epochs in the case of MultiMLPs is set as 1000, except for *energy_efficiency* and *QSAR_fish_toxicity*, where this is changed to 5000. Any model-specific hyperparameter we did not specify in this paper remains at the implementation’s default value (e.g., the number of leaves in XGBoost [50]). Along with the supplementary code, we provide two additional CSV files: one for the optimal hyperparameters of SEMF models and the other for the results and hyperparameters of all 330 runs.

Additional conditions are applied only for experiments with missing data. Datasets *california_housing*, *cpu_activity*, *miami_housing*, and *naval_propulsion_plant*—have a PATIENCE of five to expedite the training process. Additionally, for *california_housing* and *cpu_activity*, the R_{infer} value is set to 30, while for all the other datasets, it is set to 50. We do this to ensure efficient computation, speed, and memory usage (especially for the GPU).

For training MultiXGBs and MultiETs, the computations are performed in parallel using CPU cores (Intel® Core™ i9-13900KF). For MultiMLPs, they are done on a GPU (NVIDIA® GeForce RTX™ 4090). The GPU is also consistently used for the missing data simulator and training p_{ξ} . All the computations are done on a machine with 32 GB of memory. The code provides further details on hardware and reproducibility.

D Metrics for prediction intervals

D.1 Common metrics

The most common metrics for evaluating prediction intervals [52, 53] are:

- Prediction Interval Coverage Probability (PICP): This metric assesses the proportion of times the true value of the target variable falls within the constructed prediction intervals. For a set of test examples $(x_1, y_1), \dots, (x_N, y_N)$, a given level of confidence α , and their corresponding prediction intervals I_1, \dots, I_N , the PICP is calculated as:

$$\text{PICP} = \frac{1}{N} \sum_{i=1}^N \mathbb{1}(y_i \in [L_i, U_i]), \quad (21)$$

where U_i and L_i are the upper and lower bounds of the predicted values for the i -th instance. y_i is the actual value of the i -th test example, and $\mathbb{1}$ is the indicator function, which equals 1 if y_i is in the interval $[L_i, U_i]$ and 0 otherwise. $0 \leq \text{PICP} \leq 1$ where PICP closer to 1 and higher than the confidence level α is favored.

- Mean Prediction Interval Width (MPIW): The average width is computed as

$$\text{MPIW} = \frac{1}{N} \sum_{i=1}^N (U_i - L_i), \quad (22)$$

which shows the sharpness or uncertainty, where $0 \leq \text{MPIW} < \infty$ and MPIW close to 0 is preferred.

- Normalized Mean Prediction Interval Width (NMPIW): Since MPIW varies by dataset, it can be normalized by the range of the target variable

$$\text{NMPIW} = \frac{\text{MPIW}}{\max(y) - \min(y)} \quad (23)$$

where $\max(y)$ and $\min(y)$ are the maximum and minimum values of the target variable, respectively. The interpretation remains the same as MPIW.

D.2 Impact of relative metrics for modeling

As our primary focus is on interval prediction, configurations demonstrating the most significant improvements in ΔCWR and ΔPICP are prioritized when selecting the optimal hyper-parameters. Furthermore, both ΔPICP and ΔCWR must be positive, indicating that we must at least have the same reliability of the baseline (PICP) with better or same interval ratios (CWR). In instances where no configuration meets the initial improvement criteria for both metrics, we relax the requirement for positive ΔPICP to accept values greater than -5% and subsequently -10%, allowing us to consider configurations where SEMF significantly improves CWR, even if the PICP improvement is less marked but remains within an acceptable range for drawing comparisons.

E Full results

Table 6: Test results for MultiXGBs with complete data at 95% quantiles for seeds 0, 10, 20, 30, 40, with rows ordered by seed (ascending). Performance over the baseline is highlighted in bold.

DATASET	INTERVAL PREDICTIONS						POINT PREDICTIONS		
	RELATIVE			ABSOLUTE			RELATIVE		ABSOLUTE
	ΔCWR	ΔPICP	ΔNMPIW	PICP	MPIW	NMPIW	ΔRMSE	ΔMAE	R^2
SPACE_GA	-1%	6%	-7%	0.88	1.85	0.20	-10%	-13%	0.60
SPACE_GA	-4%	5%	-9%	0.89	1.85	0.20	-8%	-10%	0.59
SPACE_GA	1%	9%	-8%	0.90	1.76	0.19	-10%	-10%	0.62
SPACE_GA	-7%	5%	-12%	0.90	1.92	0.21	-8%	-10%	0.59
SPACE_GA	8%	3%	4%	0.87	1.61	0.17	-9%	-8%	0.60
CPU_ACTIVITY	27%	7%	16%	0.88	0.37	0.07	21%	0%	0.98
CPU_ACTIVITY	33%	11%	17%	0.89	0.37	0.07	23%	-2%	0.98
CPU_ACTIVITY	30%	10%	15%	0.88	0.36	0.07	20%	-5%	0.98
CPU_ACTIVITY	16%	9%	7%	0.89	0.38	0.07	20%	-3%	0.98
CPU_ACTIVITY	18%	9%	8%	0.90	0.38	0.07	22%	2%	0.98
NAVAL_PROPULSION_PLANT	176%	8%	61%	0.96	0.39	0.12	-20%	-14%	0.99
NAVAL_PROPULSION_PLANT	151%	7%	58%	0.96	0.40	0.12	-9%	-15%	0.99
NAVAL_PROPULSION_PLANT	136%	8%	54%	0.96	0.40	0.12	-15%	-12%	0.99
NAVAL_PROPULSION_PLANT	156%	7%	58%	0.95	0.38	0.11	-12%	-9%	0.99
NAVAL_PROPULSION_PLANT	161%	9%	58%	0.96	0.38	0.11	-15%	-11%	0.99
MIAMI_HOUSING	50%	-5%	37%	0.82	0.46	0.06	3%	-1%	0.91
MIAMI_HOUSING	65%	-7%	44%	0.83	0.45	0.06	4%	1%	0.91
MIAMI_HOUSING	62%	-10%	44%	0.81	0.44	0.06	7%	7%	0.90
MIAMI_HOUSING	62%	-7%	43%	0.82	0.44	0.05	9%	5%	0.91
MIAMI_HOUSING	65%	-9%	45%	0.81	0.44	0.05	-4%	0%	0.90
KIN8NM	12%	4%	8%	0.89	1.88	0.37	-17%	-20%	0.64
KIN8NM	11%	5%	6%	0.89	1.91	0.37	-21%	-22%	0.63
KIN8NM	11%	5%	6%	0.90	1.92	0.38	-19%	-21%	0.64
KIN8NM	5%	7%	-3%	0.91	2.06	0.40	-20%	-23%	0.62
KIN8NM	8%	3%	5%	0.88	1.91	0.37	-21%	-24%	0.62
CONCRETE_COMPRESSIVE_STRENGTH	7%	34%	-26%	0.91	1.26	0.26	-34%	-52%	0.86
CONCRETE_COMPRESSIVE_STRENGTH	13%	22%	-7%	0.89	1.25	0.25	-29%	-52%	0.84
CONCRETE_COMPRESSIVE_STRENGTH	13%	18%	-5%	0.91	1.20	0.24	-21%	-34%	0.86
CONCRETE_COMPRESSIVE_STRENGTH	20%	31%	-9%	0.93	1.27	0.26	-16%	-22%	0.86
CONCRETE_COMPRESSIVE_STRENGTH	14%	26%	-10%	0.90	1.25	0.25	-28%	-39%	0.83
CARS	35%	14%	16%	0.89	0.67	0.11	-5%	-1%	0.95
CARS	16%	10%	5%	0.85	0.67	0.11	-4%	-4%	0.95
CARS	13%	20%	-6%	0.91	0.78	0.13	-2%	0%	0.95
CARS	12%	16%	-4%	0.88	0.68	0.11	2%	5%	0.96
CARS	16%	18%	-2%	0.91	0.71	0.12	-7%	-4%	0.95
ENERGY_EFFICIENCY	255%	24%	64%	0.88	0.14	0.04	-50%	-29%	1.00
ENERGY_EFFICIENCY	320%	19%	71%	0.91	0.14	0.04	-3%	-13%	1.00
ENERGY_EFFICIENCY	257%	17%	67%	0.90	0.16	0.05	-21%	-31%	1.00
ENERGY_EFFICIENCY	322%	16%	73%	0.85	0.12	0.04	17%	16%	1.00
ENERGY_EFFICIENCY	78%	34%	26%	0.89	0.22	0.06	-17%	-22%	1.00
CALIFORNIA_HOUSING	24%	1%	18%	0.88	1.19	0.28	-2%	-3%	0.81
CALIFORNIA_HOUSING	28%	1%	21%	0.88	1.16	0.28	0%	-1%	0.82
CALIFORNIA_HOUSING	33%	0%	25%	0.89	1.19	0.28	0%	0%	0.81
CALIFORNIA_HOUSING	30%	1%	22%	0.87	1.16	0.28	-1%	-1%	0.82
CALIFORNIA_HOUSING	38%	-2%	29%	0.87	1.15	0.27	-1%	-2%	0.81
AIRFOIL_SELF_NOISE	68%	6%	37%	0.83	0.80	0.17	-41%	-43%	0.89
AIRFOIL_SELF_NOISE	134%	5%	55%	0.81	0.59	0.13	-18%	-18%	0.93
AIRFOIL_SELF_NOISE	13%	-3%	15%	0.72	1.10	0.23	-109%	-138%	0.78
AIRFOIL_SELF_NOISE	38%	20%	13%	0.91	1.12	0.24	-73%	-76%	0.85
AIRFOIL_SELF_NOISE	51%	-6%	38%	0.76	0.84	0.18	-82%	-93%	0.86
QSAR_FISH_TOXICITY	11%	17%	-5%	0.77	1.48	0.23	3%	3%	0.53
QSAR_FISH_TOXICITY	11%	9%	3%	0.75	1.42	0.22	8%	7%	0.58
QSAR_FISH_TOXICITY	4%	8%	-5%	0.77	1.48	0.23	4%	3%	0.57
QSAR_FISH_TOXICITY	10%	9%	1%	0.77	1.45	0.23	-2%	-1%	0.54
QSAR_FISH_TOXICITY	13%	15%	-1%	0.74	1.48	0.23	0%	-6%	0.52

Table 7: Test results for MultiETs with complete data at 95% quantiles for seeds 0, 10, 20, 30, 40, with rows ordered by seed (ascending). Performance over the baseline is highlighted in bold.

DATASET	INTERVAL PREDICTIONS						POINT PREDICTIONS		
	RELATIVE			ABSOLUTE			RELATIVE		ABSOLUTE
	Δ CWR	Δ PICP	Δ NMPIW	PICP	MPIW	NMPIW	Δ RMSE	Δ MAE	R ²
SPACE_GA	3%	0%	3%	0.92	2.15	0.23	-19%	-24%	0.51
SPACE_GA	8%	-1%	9%	0.91	2.04	0.22	-15%	-18%	0.54
SPACE_GA	10%	-1%	10%	0.91	2.04	0.22	-16%	-17%	0.54
SPACE_GA	11%	-2%	11%	0.91	2.01	0.22	-14%	-17%	0.55
SPACE_GA	12%	-3%	13%	0.90	1.96	0.21	-14%	-15%	0.55
CPU_ACTIVITY	24%	-8%	26%	0.91	0.48	0.09	-15%	-22%	0.98
CPU_ACTIVITY	24%	-8%	25%	0.91	0.49	0.09	-17%	-22%	0.97
CPU_ACTIVITY	30%	-9%	30%	0.90	0.45	0.09	-13%	-18%	0.98
CPU_ACTIVITY	29%	-8%	28%	0.90	0.47	0.09	-13%	-18%	0.98
CPU_ACTIVITY	27%	-8%	27%	0.91	0.48	0.09	-14%	-20%	0.98
NAVAL_PROPULSION_PLANT	265%	-9%	75%	0.91	0.58	0.17	-268%	-371%	0.97
NAVAL_PROPULSION_PLANT	205%	-9%	70%	0.90	0.69	0.20	-332%	-419%	0.96
NAVAL_PROPULSION_PLANT	178%	-9%	67%	0.91	0.74	0.22	-382%	-464%	0.95
NAVAL_PROPULSION_PLANT	198%	-9%	69%	0.91	0.69	0.20	-336%	-422%	0.96
NAVAL_PROPULSION_PLANT	248%	-10%	74%	0.90	0.58	0.17	-283%	-368%	0.97
MIAMI_HOUSING	70%	-12%	48%	0.86	0.66	0.08	-12%	-22%	0.90
MIAMI_HOUSING	63%	-12%	46%	0.86	0.68	0.08	-9%	-21%	0.90
MIAMI_HOUSING	68%	-13%	48%	0.86	0.65	0.08	-9%	-20%	0.90
MIAMI_HOUSING	71%	-13%	49%	0.86	0.63	0.08	-7%	-18%	0.90
MIAMI_HOUSING	72%	-12%	49%	0.86	0.65	0.08	-12%	-21%	0.89
KIN8NM	12%	-9%	19%	0.88	2.20	0.43	-32%	-36%	0.50
KIN8NM	9%	-9%	17%	0.88	2.28	0.45	-36%	-40%	0.46
KIN8NM	11%	-10%	18%	0.88	2.24	0.44	-34%	-37%	0.49
KIN8NM	9%	-9%	16%	0.89	2.29	0.45	-34%	-36%	0.49
KIN8NM	7%	-9%	15%	0.88	2.33	0.46	-37%	-40%	0.47
CONCRETE_COMPRESSIVE_STRENGTH	25%	-15%	32%	0.79	1.02	0.21	-59%	-85%	0.78
CONCRETE_COMPRESSIVE_STRENGTH	9%	-12%	19%	0.81	1.19	0.24	-71%	-96%	0.76
CONCRETE_COMPRESSIVE_STRENGTH	4%	-11%	14%	0.83	1.22	0.25	-62%	-92%	0.77
CONCRETE_COMPRESSIVE_STRENGTH	-2%	-9%	8%	0.83	1.31	0.27	-77%	-110%	0.74
CONCRETE_COMPRESSIVE_STRENGTH	11%	-12%	20%	0.81	1.14	0.23	-64%	-88%	0.77
CARS	3%	15%	-11%	0.83	0.54	0.09	3%	2%	0.95
CARS	16%	18%	-2%	0.85	0.52	0.09	3%	0%	0.95
CARS	21%	13%	7%	0.80	0.47	0.08	4%	-1%	0.95
CARS	6%	17%	-10%	0.84	0.56	0.10	-2%	0%	0.94
CARS	10%	17%	-7%	0.85	0.54	0.09	8%	5%	0.95
ENERGY_EFFICIENCY	-3%	-3%	0%	0.63	0.07	0.02	3%	0%	1.00
ENERGY_EFFICIENCY	-3%	1%	-5%	0.66	0.08	0.02	7%	3%	1.00
ENERGY_EFFICIENCY	-14%	9%	-29%	0.70	0.09	0.03	0%	0%	1.00
ENERGY_EFFICIENCY	2%	-11%	14%	0.59	0.07	0.02	-3%	-2%	1.00
ENERGY_EFFICIENCY	-5%	1%	-5%	0.65	0.08	0.02	6%	0%	1.00
CALIFORNIA_HOUSING	33%	-7%	30%	0.91	1.71	0.41	-14%	-19%	0.72
CALIFORNIA_HOUSING	28%	-7%	27%	0.91	1.74	0.41	-16%	-22%	0.70
CALIFORNIA_HOUSING	34%	-7%	31%	0.90	1.67	0.40	-14%	-20%	0.72
CALIFORNIA_HOUSING	29%	-7%	28%	0.91	1.72	0.41	-16%	-22%	0.71
CALIFORNIA_HOUSING	31%	-8%	30%	0.90	1.69	0.40	-15%	-20%	0.71
AIRFOIL_SELF_NOISE	8%	-21%	27%	0.77	1.20	0.26	-168%	-189%	0.74
AIRFOIL_SELF_NOISE	-16%	-14%	-3%	0.84	1.68	0.36	-170%	-214%	0.67
AIRFOIL_SELF_NOISE	20%	-8%	24%	0.89	1.22	0.26	-95%	-105%	0.84
AIRFOIL_SELF_NOISE	62%	-18%	49%	0.81	0.82	0.18	-57%	-81%	0.89
AIRFOIL_SELF_NOISE	18%	-13%	26%	0.86	1.19	0.25	-93%	-118%	0.85
QSAR_FISH_TOXICITY	11%	-10%	19%	0.81	1.82	0.28	-6%	-13%	0.53
QSAR_FISH_TOXICITY	13%	-10%	21%	0.82	1.79	0.28	-5%	-11%	0.54
QSAR_FISH_TOXICITY	14%	-10%	21%	0.82	1.82	0.28	-8%	-12%	0.51
QSAR_FISH_TOXICITY	11%	-8%	17%	0.82	1.79	0.28	-5%	-11%	0.53
QSAR_FISH_TOXICITY	9%	-8%	16%	0.84	1.84	0.29	-6%	-10%	0.52

Table 8: Test results for MultiMLPs with complete data at 95% quantiles for seeds 0, 10, 20, 30, 40, with rows ordered by seed (ascending). Performance over the baseline is highlighted in bold.

DATASET	INTERVAL PREDICTIONS						POINT PREDICTIONS		
	RELATIVE			ABSOLUTE			RELATIVE		ABSOLUTE
	Δ CWR	Δ PICP	Δ NMPIW	PICP	MPIW	NMPIW	Δ RMSE	Δ MAE	R ²
SPACE_GA	7%	-4%	10%	0.79	1.22	0.13	-1%	-1%	0.75
SPACE_GA	8%	2%	5%	0.82	1.25	0.14	0%	0%	0.76
SPACE_GA	7%	4%	3%	0.83	1.27	0.14	-3%	-3%	0.74
SPACE_GA	8%	-1%	8%	0.79	1.24	0.14	0%	-1%	0.74
SPACE_GA	9%	-2%	10%	0.81	1.27	0.14	1%	0%	0.76
CPU_ACTIVITY	8%	-11%	16%	0.72	0.25	0.05	6%	5%	0.98
CPU_ACTIVITY	14%	-15%	25%	0.68	0.23	0.04	8%	5%	0.98
CPU_ACTIVITY	8%	-8%	15%	0.73	0.24	0.04	8%	7%	0.98
CPU_ACTIVITY	5%	-3%	8%	0.74	0.25	0.05	6%	5%	0.98
CPU_ACTIVITY	6%	-8%	12%	0.70	0.24	0.04	4%	2%	0.98
NAVAL_PROPULSION_PLANT	50%	0%	34%	0.92	0.19	0.06	-44%	-48%	1.00
NAVAL_PROPULSION_PLANT	20%	0%	17%	0.93	0.20	0.06	-35%	-13%	1.00
NAVAL_PROPULSION_PLANT	3%	1%	3%	0.92	0.26	0.08	-51%	-45%	0.99
NAVAL_PROPULSION_PLANT	3%	3%	0%	0.94	0.23	0.07	-86%	-63%	1.00
NAVAL_PROPULSION_PLANT	29%	-6%	27%	0.91	0.23	0.07	-9%	-11%	1.00
MIAMI_HOUSING	13%	-2%	13%	0.78	0.37	0.05	-2%	7%	0.91
MIAMI_HOUSING	10%	3%	6%	0.81	0.40	0.05	-6%	1%	0.91
MIAMI_HOUSING	14%	1%	10%	0.82	0.42	0.05	-2%	3%	0.92
MIAMI_HOUSING	8%	1%	7%	0.82	0.43	0.05	-1%	4%	0.91
MIAMI_HOUSING	3%	6%	-4%	0.83	0.44	0.06	-4%	6%	0.91
KIN8NM	-5%	9%	-15%	0.81	0.69	0.13	6%	5%	0.93
KIN8NM	15%	1%	12%	0.78	0.62	0.12	7%	7%	0.93
KIN8NM	2%	4%	-2%	0.82	0.67	0.13	10%	10%	0.94
KIN8NM	2%	14%	-12%	0.83	0.69	0.14	10%	6%	0.94
KIN8NM	-3%	12%	-15%	0.83	0.71	0.14	4%	5%	0.93
CONCRETE_COMPRESSIVE_STRENGTH	89%	-14%	54%	0.62	0.30	0.06	4%	10%	0.90
CONCRETE_COMPRESSIVE_STRENGTH	82%	-21%	57%	0.55	0.29	0.06	9%	15%	0.91
CONCRETE_COMPRESSIVE_STRENGTH	120%	-17%	62%	0.60	0.28	0.06	18%	19%	0.92
CONCRETE_COMPRESSIVE_STRENGTH	100%	-33%	66%	0.52	0.27	0.06	9%	12%	0.91
CONCRETE_COMPRESSIVE_STRENGTH	101%	-30%	65%	0.52	0.28	0.06	18%	20%	0.91
CARS	10%	3%	7%	0.77	0.38	0.06	-4%	5%	0.95
CARS	-23%	28%	-65%	0.88	0.54	0.09	1%	1%	0.96
CARS	16%	-4%	17%	0.65	0.29	0.05	-6%	-2%	0.95
CARS	2%	-6%	8%	0.68	0.34	0.06	-2%	-1%	0.95
CARS	-5%	8%	-13%	0.81	0.45	0.08	-5%	-2%	0.95
ENERGY_EFFICIENCY	93%	59%	17%	0.70	0.07	0.02	37%	38%	1.00
ENERGY_EFFICIENCY	83%	27%	29%	0.61	0.06	0.02	28%	32%	1.00
ENERGY_EFFICIENCY	109%	28%	39%	0.64	0.06	0.02	35%	32%	1.00
ENERGY_EFFICIENCY	65%	26%	24%	0.58	0.07	0.02	31%	31%	1.00
ENERGY_EFFICIENCY	60%	-15%	47%	0.58	0.06	0.02	31%	32%	1.00
CALIFORNIA_HOUSING	-13%	9%	-25%	0.90	1.33	0.32	7%	8%	0.81
CALIFORNIA_HOUSING	-15%	6%	-24%	0.89	1.27	0.30	7%	9%	0.82
CALIFORNIA_HOUSING	-11%	9%	-23%	0.90	1.29	0.31	8%	11%	0.82
CALIFORNIA_HOUSING	-14%	8%	-26%	0.89	1.31	0.31	7%	8%	0.81
CALIFORNIA_HOUSING	-18%	9%	-33%	0.90	1.32	0.32	7%	9%	0.82
AIRFOIL_SELF_NOISE	140%	-10%	62%	0.74	0.34	0.07	18%	18%	0.97
AIRFOIL_SELF_NOISE	42%	9%	23%	0.73	0.34	0.07	11%	9%	0.97
AIRFOIL_SELF_NOISE	43%	-1%	31%	0.77	0.36	0.08	22%	22%	0.97
AIRFOIL_SELF_NOISE	39%	3%	26%	0.73	0.35	0.07	17%	12%	0.97
AIRFOIL_SELF_NOISE	105%	-2%	52%	0.77	0.38	0.08	21%	19%	0.97
QSAR_FISH_TOXICITY	-6%	8%	-14%	0.72	1.40	0.22	-4%	6%	0.52
QSAR_FISH_TOXICITY	0%	17%	-17%	0.82	1.50	0.23	6%	11%	0.54
QSAR_FISH_TOXICITY	-5%	8%	-13%	0.77	1.57	0.24	0%	-1%	0.57
QSAR_FISH_TOXICITY	-8%	13%	-23%	0.78	1.51	0.23	10%	9%	0.61
QSAR_FISH_TOXICITY	-12%	10%	-25%	0.73	1.49	0.23	5%	11%	0.51

Table 9: Test results for MultiXGBs with 50% missing data at 95% quantiles for seeds 0, 10, 20, 30, 40, with rows ordered by seed (ascending). Performance over the baseline is highlighted in bold.

DATASET	INTERVAL PREDICTIONS						POINT PREDICTIONS		
	RELATIVE			ABSOLUTE			RELATIVE		ABSOLUTE
	Δ CWR	Δ PICP	Δ NMPIW	PICP	MPIW	NMPIW	Δ RMSE	Δ MAE	R ²
SPACE_GA	-12%	5%	-20%	0.87	2.25	0.24	-11%	-13%	0.35
SPACE_GA	-9%	6%	-18%	0.87	2.15	0.23	-12%	-11%	0.44
SPACE_GA	3%	6%	-5%	0.85	1.90	0.21	-1%	-6%	0.46
SPACE_GA	-8%	4%	-14%	0.89	2.06	0.22	-5%	-11%	0.54
SPACE_GA	0%	1%	-4%	0.82	1.88	0.20	-6%	-6%	0.45
CPU_ACTIVITY	2%	2%	-1%	0.79	0.58	0.11	-30%	-30%	0.73
CPU_ACTIVITY	9%	7%	-12%	0.87	0.61	0.12	-7%	-23%	0.94
CPU_ACTIVITY	-41%	27%	-127%	0.96	1.17	0.22	-1%	-26%	0.81
CPU_ACTIVITY	-8%	14%	-34%	0.94	0.78	0.15	36%	5%	0.88
CPU_ACTIVITY	12%	8%	-12%	0.91	0.66	0.12	-2%	-11%	0.81
NAVAL_PROPULSION_PLANT	82%	-9%	47%	0.76	0.64	0.19	-30%	-42%	0.83
NAVAL_PROPULSION_PLANT	121%	-13%	59%	0.76	0.65	0.19	5%	-6%	0.84
NAVAL_PROPULSION_PLANT	127%	-13%	58%	0.73	0.66	0.20	6%	6%	0.76
NAVAL_PROPULSION_PLANT	134%	-21%	63%	0.64	0.52	0.15	-7%	-11%	0.70
NAVAL_PROPULSION_PLANT	58%	-25%	53%	0.62	0.64	0.19	-45%	-90%	0.73
MIAMI_HOUSING	16%	-6%	13%	0.84	0.86	0.11	-4%	-4%	0.72
MIAMI_HOUSING	-9%	4%	-22%	0.90	0.94	0.12	-14%	-20%	0.79
MIAMI_HOUSING	25%	-11%	17%	0.72	0.60	0.07	-35%	-35%	0.54
MIAMI_HOUSING	23%	-4%	21%	0.85	0.83	0.10	-7%	-12%	0.80
MIAMI_HOUSING	25%	-9%	21%	0.78	0.63	0.08	-10%	-19%	0.76
KIN8NM	-3%	2%	-12%	0.88	2.41	0.47	0%	1%	0.40
KIN8NM	-6%	3%	-14%	0.89	2.47	0.48	-6%	-8%	0.39
KIN8NM	-4%	2%	-10%	0.88	2.48	0.48	-5%	-6%	0.37
KIN8NM	-9%	7%	-23%	0.90	2.57	0.50	-5%	-7%	0.44
KIN8NM	-3%	3%	-10%	0.87	2.38	0.47	1%	2%	0.41
CONCRETE_COMPRESSIVE_STRENGTH	-2%	0%	-6%	0.71	1.51	0.30	-19%	-22%	0.48
CONCRETE_COMPRESSIVE_STRENGTH	2%	11%	-15%	0.81	1.44	0.29	-4%	-3%	0.69
CONCRETE_COMPRESSIVE_STRENGTH	4%	11%	-12%	0.76	1.44	0.29	-15%	-24%	0.50
CONCRETE_COMPRESSIVE_STRENGTH	1%	8%	-9%	0.77	1.47	0.30	-4%	-9%	0.64
CONCRETE_COMPRESSIVE_STRENGTH	7%	8%	-7%	0.80	1.49	0.30	-37%	-44%	0.57
CARS	-3%	24%	-34%	0.85	1.34	0.23	-9%	-16%	0.75
CARS	-35%	9%	-98%	0.82	1.78	0.30	-68%	-80%	0.55
CARS	-6%	29%	-52%	0.88	1.54	0.26	-8%	-14%	0.76
CARS	-29%	32%	-90%	0.81	1.73	0.29	-28%	-39%	0.40
CARS	-5%	34%	-40%	0.92	1.49	0.25	-37%	-25%	0.81
ENERGY_EFFICIENCY	20%	15%	-13%	0.93	0.71	0.21	-37%	-39%	0.94
ENERGY_EFFICIENCY	35%	3%	23%	0.88	0.58	0.17	-15%	-24%	0.97
ENERGY_EFFICIENCY	37%	7%	19%	0.92	0.63	0.18	-16%	-44%	0.96
ENERGY_EFFICIENCY	-21%	18%	-81%	0.95	1.01	0.29	-155%	-137%	0.93
ENERGY_EFFICIENCY	-22%	14%	-66%	0.91	0.92	0.27	-705%	-520%	0.76
CALIFORNIA_HOUSING	30%	-8%	28%	0.82	1.52	0.36	-4%	-7%	0.61
CALIFORNIA_HOUSING	26%	-2%	21%	0.89	1.61	0.39	0%	1%	0.73
CALIFORNIA_HOUSING	34%	-1%	26%	0.90	1.66	0.40	-11%	-13%	0.73
CALIFORNIA_HOUSING	13%	0%	11%	0.90	1.85	0.44	-3%	-3%	0.65
CALIFORNIA_HOUSING	27%	0%	21%	0.91	1.70	0.41	-1%	-3%	0.73
AIRFOIL_SELF_NOISE	-8%	4%	-14%	0.77	1.70	0.36	-14%	-8%	0.52
AIRFOIL_SELF_NOISE	-18%	-2%	-20%	0.80	1.77	0.38	-94%	-110%	0.50
AIRFOIL_SELF_NOISE	-12%	-7%	-11%	0.70	1.86	0.40	-43%	-48%	0.19
AIRFOIL_SELF_NOISE	34%	-5%	29%	0.69	1.02	0.22	-19%	-29%	0.38
AIRFOIL_SELF_NOISE	-6%	-6%	-5%	0.71	1.58	0.34	-14%	-22%	0.43
QSAR_FISH_TOXICITY	-3%	-4%	-1%	0.68	1.56	0.24	-4%	-5%	0.38
QSAR_FISH_TOXICITY	-1%	-4%	2%	0.75	1.83	0.28	-9%	-3%	0.35
QSAR_FISH_TOXICITY	3%	9%	-8%	0.75	1.66	0.26	4%	4%	0.43
QSAR_FISH_TOXICITY	-6%	1%	-19%	0.72	1.61	0.25	-7%	-3%	0.35
QSAR_FISH_TOXICITY	-1%	-3%	-2%	0.74	1.84	0.29	-5%	-3%	0.30

Table 10: Test results for MultiETs with 50% missing data at 95% quantiles for seeds 0, 10, 20, 30, 40, with rows ordered by seed (ascending). Performance over the baseline is highlighted in bold.

DATASET	INTERVAL PREDICTIONS						POINT PREDICTIONS		
	RELATIVE			ABSOLUTE			RELATIVE		ABSOLUTE
	Δ CWR	Δ PICP	Δ NMPIW	PICP	MPIW	NMPIW	Δ RMSE	Δ MAE	R ²
SPACE_GA	7%	-6%	12%	0.86	2.17	0.23	-17%	-18%	0.30
SPACE_GA	3%	-5%	8%	0.87	2.14	0.23	-14%	-15%	0.41
SPACE_GA	2%	-5%	5%	0.88	2.23	0.24	-9%	-10%	0.41
SPACE_GA	7%	-5%	9%	0.86	2.21	0.24	-7%	-7%	0.40
SPACE_GA	-1%	-3%	0%	0.91	2.39	0.26	-14%	-18%	0.47
CPU_ACTIVITY	-8%	-5%	-8%	0.93	0.90	0.17	-36%	-46%	0.93
CPU_ACTIVITY	-8%	-6%	-4%	0.92	0.89	0.17	2%	-23%	0.87
CPU_ACTIVITY	-30%	-3%	-43%	0.94	1.33	0.25	-36%	-80%	0.73
CPU_ACTIVITY	-27%	-3%	-41%	0.94	1.21	0.23	-13%	-49%	0.74
CPU_ACTIVITY	-6%	-6%	-3%	0.91	1.00	0.19	-65%	-70%	0.67
NAVAL_PROPULSION_PLANT	55%	-22%	48%	0.77	1.29	0.38	-18%	-50%	0.64
NAVAL_PROPULSION_PLANT	55%	-10%	42%	0.89	1.52	0.45	-66%	-158%	0.79
NAVAL_PROPULSION_PLANT	54%	-15%	44%	0.84	1.44	0.42	-29%	-73%	0.74
NAVAL_PROPULSION_PLANT	67%	-16%	50%	0.83	1.29	0.38	-56%	-142%	0.74
NAVAL_PROPULSION_PLANT	57%	-20%	48%	0.78	1.38	0.41	-14%	-42%	0.66
MIAMI_HOUSING	20%	-6%	22%	0.92	1.33	0.17	-13%	-26%	0.78
MIAMI_HOUSING	32%	-16%	31%	0.79	0.87	0.11	-41%	-50%	0.48
MIAMI_HOUSING	-4%	-5%	-1%	0.92	1.39	0.17	-38%	-51%	0.67
MIAMI_HOUSING	37%	-14%	36%	0.84	0.88	0.11	-21%	-34%	0.79
MIAMI_HOUSING	16%	-7%	16%	0.89	1.30	0.16	-20%	-26%	0.65
KIN8NM	5%	-9%	13%	0.86	2.48	0.49	-10%	-12%	0.32
KIN8NM	4%	-8%	9%	0.87	2.58	0.51	-10%	-12%	0.33
KIN8NM	5%	-8%	12%	0.87	2.62	0.51	-13%	-15%	0.30
KIN8NM	8%	-11%	17%	0.84	2.41	0.47	-8%	-8%	0.30
KIN8NM	1%	-5%	6%	0.90	2.66	0.52	-14%	-18%	0.37
CONCRETE_COMPRESSIVE_STRENGTH	4%	-11%	15%	0.79	1.88	0.38	-24%	-36%	0.46
CONCRETE_COMPRESSIVE_STRENGTH	-3%	-17%	12%	0.78	1.74	0.35	-26%	-36%	0.42
CONCRETE_COMPRESSIVE_STRENGTH	4%	-12%	13%	0.81	1.83	0.37	-30%	-47%	0.56
CONCRETE_COMPRESSIVE_STRENGTH	7%	-11%	15%	0.83	1.81	0.37	-19%	-31%	0.58
CONCRETE_COMPRESSIVE_STRENGTH	-7%	-18%	9%	0.80	1.87	0.38	-76%	-99%	0.45
CARS	-18%	1%	-39%	0.89	1.29	0.22	-16%	-15%	0.81
CARS	-18%	-11%	-11%	0.84	1.39	0.23	-23%	-30%	0.72
CARS	-33%	-6%	-54%	0.84	1.63	0.28	-59%	-59%	0.60
CARS	-28%	-12%	-41%	0.80	1.27	0.21	-18%	-10%	0.59
CARS	-19%	-14%	-29%	0.79	1.48	0.25	-49%	-42%	0.59
ENERGY_EFFICIENCY	-11%	13%	-35%	0.91	0.50	0.14	-7%	-13%	0.98
ENERGY_EFFICIENCY	0%	-7%	0%	0.83	0.49	0.14	-8%	-20%	0.95
ENERGY_EFFICIENCY	-9%	-14%	0%	0.76	0.47	0.14	-112%	-137%	0.93
ENERGY_EFFICIENCY	-11%	4%	-30%	0.87	0.59	0.17	-38%	-76%	0.96
ENERGY_EFFICIENCY	-46%	2%	-114%	0.89	0.52	0.15	-198%	-176%	0.86
CALIFORNIA_HOUSING	30%	-7%	28%	0.92	2.09	0.50	-11%	-13%	0.64
CALIFORNIA_HOUSING	28%	-9%	28%	0.87	2.02	0.48	-14%	-18%	0.50
CALIFORNIA_HOUSING	13%	-6%	17%	0.92	2.24	0.53	-19%	-23%	0.64
CALIFORNIA_HOUSING	19%	-5%	20%	0.93	2.23	0.53	-12%	-16%	0.64
CALIFORNIA_HOUSING	16%	-6%	18%	0.93	2.35	0.56	-11%	-16%	0.60
AIRFOIL_SELF_NOISE	-7%	-18%	10%	0.77	2.02	0.43	-27%	-51%	0.36
AIRFOIL_SELF_NOISE	-26%	-18%	-11%	0.80	2.21	0.47	-171%	-229%	0.30
AIRFOIL_SELF_NOISE	25%	-20%	36%	0.74	1.28	0.27	-28%	-38%	0.41
AIRFOIL_SELF_NOISE	-22%	-24%	-2%	0.73	2.26	0.48	-54%	-86%	0.13
AIRFOIL_SELF_NOISE	-7%	-18%	10%	0.79	2.02	0.43	-44%	-58%	0.43
QSAR_FISH_TOXICITY	11%	-8%	15%	0.85	2.37	0.37	-11%	-10%	0.40
QSAR_FISH_TOXICITY	13%	-8%	18%	0.82	2.02	0.31	-1%	-5%	0.47
QSAR_FISH_TOXICITY	19%	-7%	22%	0.84	1.90	0.29	-3%	-3%	0.48
QSAR_FISH_TOXICITY	-3%	-15%	12%	0.76	2.02	0.32	-24%	-27%	0.25
QSAR_FISH_TOXICITY	8%	-9%	14%	0.83	2.29	0.36	-3%	-5%	0.36

Table 11: Test results for MultiMLPs with 50% missing data at 95% quantiles for seeds 0, 10, 20, 30, 40, with rows ordered by seed (ascending). Performance over the baseline is highlighted in bold.

DATASET	INTERVAL PREDICTIONS						POINT PREDICTIONS		
	RELATIVE			ABSOLUTE			RELATIVE	ABSOLUTE	
	Δ CWR	Δ PICP	Δ NMPIW	PICP	MPIW	NMPIW	Δ RMSE	Δ MAE	R ²
SPACE_GA	-12%	-16%	4%	0.68	1.50	0.16	-41%	-40%	0.15
SPACE_GA	-21%	-17%	-11%	0.64	1.41	0.15	-85%	-61%	-0.21
SPACE_GA	-5%	-14%	6%	0.65	1.30	0.14	-21%	-20%	0.37
SPACE_GA	-9%	-13%	4%	0.70	1.50	0.16	-28%	-25%	0.35
SPACE_GA	-9%	-13%	1%	0.73	1.49	0.16	-25%	-26%	0.38
CPU_ACTIVITY	-38%	14%	-89%	0.87	0.75	0.14	14%	1%	0.92
CPU_ACTIVITY	-60%	32%	-240%	0.94	1.08	0.20	-20%	-17%	0.78
CPU_ACTIVITY	-67%	36%	-355%	0.95	1.50	0.28	-30%	-34%	0.72
CPU_ACTIVITY	-24%	-2%	-28%	0.68	0.39	0.07	-3%	-16%	0.78
CPU_ACTIVITY	-63%	28%	-251%	0.85	1.13	0.21	-37%	-49%	0.54
NAVAL_PROPULSION_PLANT	-41%	0%	-70%	0.63	0.85	0.25	-62%	-68%	-0.21
NAVAL_PROPULSION_PLANT	-53%	-13%	-87%	0.82	1.60	0.47	-141%	-163%	0.50
NAVAL_PROPULSION_PLANT	-48%	-3%	-85%	0.72	1.23	0.36	-99%	-94%	0.16
NAVAL_PROPULSION_PLANT	-88%	-61%	-210%	0.29	1.10	0.33	-215%	-562%	-0.85
NAVAL_PROPULSION_PLANT	-33%	4%	-55%	0.70	1.04	0.31	-24%	-27%	0.27
MIAMI_HOUSING	-48%	22%	-148%	0.93	1.33	0.17	-21%	-20%	0.74
MIAMI_HOUSING	-54%	27%	-202%	0.89	1.33	0.17	-41%	-48%	0.53
MIAMI_HOUSING	-19%	11%	-40%	0.84	0.75	0.09	-18%	-19%	0.75
MIAMI_HOUSING	-17%	6%	-32%	0.82	0.69	0.09	-23%	-22%	0.77
MIAMI_HOUSING	-28%	1%	-39%	0.76	0.82	0.10	-24%	-32%	0.57
KIN8NM	-7%	-5%	-3%	0.75	1.67	0.33	-12%	-10%	0.39
KIN8NM	-11%	-6%	-8%	0.77	1.80	0.35	-20%	-22%	0.36
KIN8NM	-19%	-4%	-19%	0.77	1.88	0.37	-20%	-19%	0.31
KIN8NM	-4%	-2%	-5%	0.77	1.68	0.33	-3%	0%	0.43
KIN8NM	-15%	-9%	-8%	0.78	1.79	0.35	-26%	-24%	0.36
CONCRETE_COMPRESSIVE_STRENGTH	-15%	5%	-26%	0.74	1.53	0.31	-9%	-6%	0.51
CONCRETE_COMPRESSIVE_STRENGTH	-5%	-38%	34%	0.40	0.57	0.12	-10%	-10%	0.46
CONCRETE_COMPRESSIVE_STRENGTH	-32%	21%	-80%	0.84	1.69	0.34	-5%	-9%	0.60
CONCRETE_COMPRESSIVE_STRENGTH	2%	-53%	54%	0.27	0.39	0.08	-20%	-23%	0.52
CONCRETE_COMPRESSIVE_STRENGTH	-25%	0%	-33%	0.76	1.37	0.28	-15%	-13%	0.59
CARS	-50%	38%	-176%	0.93	1.62	0.27	-36%	-38%	0.75
CARS	-44%	49%	-169%	0.93	1.55	0.26	-3%	-5%	0.75
CARS	-53%	32%	-232%	0.94	2.04	0.34	-34%	-33%	0.70
CARS	-49%	44%	-223%	0.89	1.59	0.27	-32%	-15%	0.48
CARS	-57%	51%	-257%	0.93	1.90	0.32	-32%	-37%	0.63
ENERGY_EFFICIENCY	-35%	4%	-68%	0.81	0.43	0.13	-8%	1%	0.97
ENERGY_EFFICIENCY	-12%	25%	-47%	0.60	0.27	0.08	8%	2%	0.92
ENERGY_EFFICIENCY	-19%	-14%	-5%	0.57	0.31	0.09	-1%	-32%	0.93
ENERGY_EFFICIENCY	-18%	7%	-29%	0.83	0.50	0.14	-8%	6%	0.96
ENERGY_EFFICIENCY	20%	26%	-3%	0.51	0.12	0.03	14%	18%	0.98
CALIFORNIA_HOUSING	-16%	1%	-20%	0.88	1.76	0.42	-7%	-3%	0.63
CALIFORNIA_HOUSING	-14%	4%	-25%	0.83	1.66	0.40	-4%	-3%	0.54
CALIFORNIA_HOUSING	-9%	0%	-10%	0.89	1.79	0.43	-1%	0%	0.68
CALIFORNIA_HOUSING	-20%	5%	-30%	0.90	1.91	0.45	-2%	-1%	0.65
CALIFORNIA_HOUSING	-27%	10%	-52%	0.89	2.09	0.50	-8%	-9%	0.55
AIRFOIL_SELF_NOISE	3%	-1%	0%	0.76	1.22	0.26	-3%	1%	0.54
AIRFOIL_SELF_NOISE	27%	-7%	26%	0.77	0.84	0.18	-20%	-11%	0.84
AIRFOIL_SELF_NOISE	8%	-7%	14%	0.62	0.63	0.14	-22%	-13%	0.31
AIRFOIL_SELF_NOISE	-9%	1%	-12%	0.76	1.44	0.31	-23%	-20%	0.44
AIRFOIL_SELF_NOISE	-20%	6%	-33%	0.83	1.62	0.35	-9%	-1%	0.62
QSAR_FISH_TOXICITY	-17%	-1%	-22%	0.75	1.89	0.29	-21%	-28%	0.28
QSAR_FISH_TOXICITY	-24%	9%	-45%	0.79	1.97	0.31	-8%	-9%	0.44
QSAR_FISH_TOXICITY	-19%	0%	-23%	0.70	1.56	0.24	-6%	-8%	0.39
QSAR_FISH_TOXICITY	-17%	16%	-41%	0.76	1.72	0.27	-21%	-17%	0.28
QSAR_FISH_TOXICITY	-9%	8%	-18%	0.81	1.98	0.31	-10%	-9%	0.32

F Example of learning with non-normality

To illustrate how SEMF adapts to non-normal outcomes, we provide an example from the *naval_propulsion_plant dataset* [57]. Figure 2 shows the distribution of the ground-truth y variable which in this case is `gt_compressor_decay_state_coefficient`. The values are uniformly distributed, and we only standardize the values without changing the shape of the distribution.

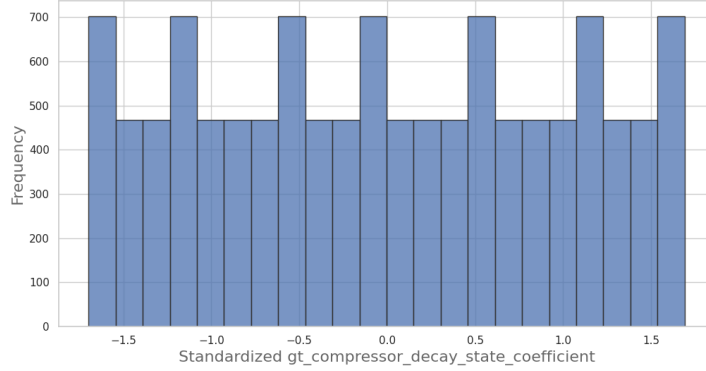


Figure 2: Distribution of the standardized outcome (y) variable for the *naval_propulsion_plant* dataset which shows that y is uniformly distributed prior to any training.

After training our SEMF model under the normality assumption with the ideal hyper-parameters (and a seed of 0), sampling from a normal distribution for the z dimension, we infer on some randomly sampled test instances that provide us with the prediction intervals in Figure 3. The ‘SEMF intervals’ can be compared with XGBoost quantile regression, constituting our baseline. This figure shows that SEMF’s predicted intervals are better than the baseline. This plot alone does not tell us much about the predicted output distribution. Therefore, we provide Figure 4. The last plot shows that for a handful of the instances, the predicted values can take any shape and are not necessarily normal.

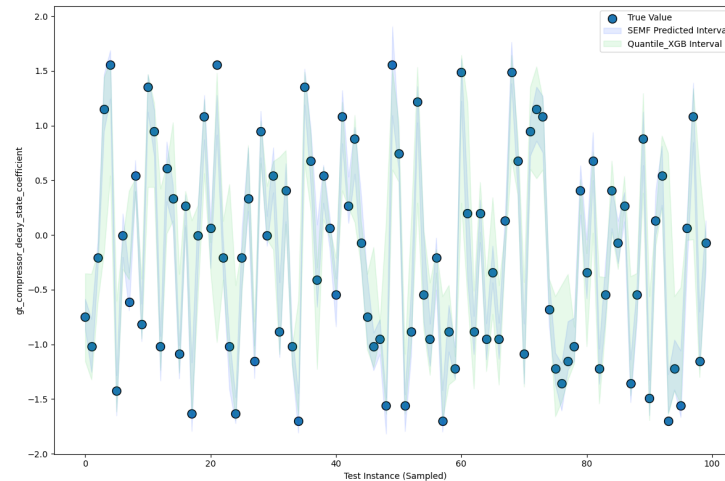


Figure 3: Predicted intervals and true values on 100 randomly selected test samples for SEMF MultiXGBs and XGBoost quantile regression with complete data at 95% quantiles (according to Eq 13).

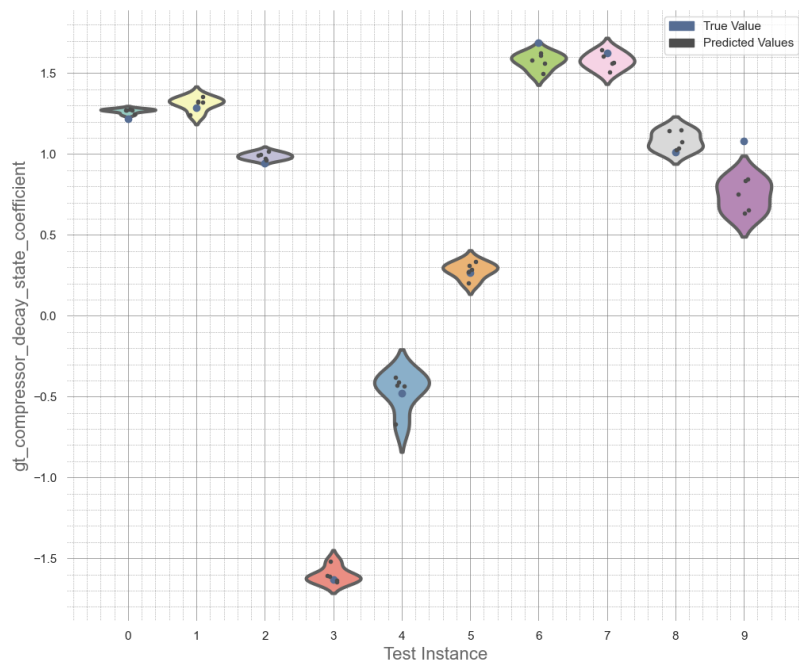


Figure 4: Violin plot for the first ten instances of the test set where both the ground truth and 50 values inferred by SEMF (according to Eq 12) are generated for each instance. We have added jitter here, so the points do not perfectly align along the x-axis.